Dissertation

The role of microRNA-142-3p in uremic vascular media calcification

submitted by

Dr. med. Máté Csaba KÉTSZERI

for the Academic Degree of

Doctor of Philosophy

(PhD)

at the

Medical University of Graz

Clinical Division of Nephrology

Department of Internal Medicine

under the supervision of

Univ.-Prof. Dr.med.univ. Alexander R. Rosenkranz

2019

Statutory Declaration

I hereby declare that this thesis is my own original work and that I have fully acknowledged by name all of those individuals and organisations that have contributed to the research for this thesis. Due acknowledgement has been made in the text to all other material used. Throughout this thesis and in all related publications I followed the "Standards of Good Scientific Practice and Ombuds Committee at the Medical University of Graz".

Graz, June 2019

Disclosures

Parts of this thesis have been published in peer-reviewed journals. Permission for the reuse of the scientific articles was obtained via the open access agreements of the publishers.

The dissertation is based on the following publication:

Ketszeri M, Kirsch A, Frauscher B, Moschovaki-Filippidou F, Mooslechner AA, Kirsch AH, et al. MicroRNA-142-3p improves vascular relaxation in uremia. Atherosclerosis. 2019;280:28-36. (1)

All co-authors gave their consent to re-use data from the publications within this thesis.

This thesis project was funded by the Austrian Science Fund (FWF) within the PhD program Molecular Medicine (MolMed).

Acknowledgement

I am grateful for all the help, advice and guidance that my supervisors, Kathrin Eller, Philipp Eller and Alexander Rosenkranz provided me throughout my studies.

I thank all the help and assistance I got from my colleagues in the laboratory: Katharina Artinger, Ida Aringer, Alexander Kirsch, Corinna Schabhüttl and Kerstin Schweighofer.

I am thankful to Barbara Küberl and Viktoria Trunk for all their help with the bureaucratic issues.

Special thanks to Foteini Moschovaki-Filippidou, Bianca Frauscher and Agnes Mooslechner for all the conversations, help and support. The most valuable thing I gained during my years in Graz was their friendship.

Table of contents

Abbreviations

ACh	acetycholine
ADPKD	autosomal dominant polycystic kidney disease
Ago2	Argonaute 2
BP	blood pressure
BSA	bovine serum albumin
BUN	blood urea nitrogen
cfPWV	carotid-femoral pulsewave velocity
CKD	chronic kidney disease
CKD-MBD	chronic kidney disease – mineral and bone disorder
CT	computed tomography
CVD	cardiovascular disease
DBA/2	dilute brown, non-agouti mouse strain
DBA/2NCrl	dilute brown, non-agouti mouse strain
DMEM	Dulbecco's modified Eagle's medium
DOPC	1,2-dioleoyl-*sn*-glycero-3-phosphocholine
ECG	electrocardiography
EGFR	epidermal growth factor receptor
ELISA	enzyme-linked immunosorbent assay
eNOS	endothelial nitric oxyde synthase
ESRD	end-stage renal disease
FCS	fetal calf serum
GalNAc	*N*-acetyl-D-galactosamine
GAPDH	glyceraldehyde 3-phosphate dehydrogenase
GFR	glomerular filtration rate
HD	hemodialysis
HNO_3	nitric acid
HPD	high phosphate diet
HRP	horseradish peroxidase
KDIGO	Kidney Disease: Improving Global outcomes
KPSS	physiological salt solution with 60mM KCl

KTx	kidney transplantation
L-NNA	Nω-nitro-L-arginine
MAP	mean arterial pressure
miR	microRNA
miRNA	microRNA
NE	norepinephrine
NO	nitric oxide
NSAID	nonsteroidal anti-inflammatory drug
NSCLC	non-small-cell lung carcinoma
PAS	periodic acid - Schiff
PBS	phosphate-buffered saline
PD	peritoneal dialysis
PEG	poly(ethylene glycol)
PEI	polyethylenimine
PGI2	prostacyclin
PKD	polycystic kidney disease
PLGA	poly(lactide-co-glycolide)
PSS	physiological salt solution
PVDF	polyvinylidene difluoride
RISC	RNA-induced silencing complex
ROS	reactive oxigen species
RT-PCR	real-time polymerase chain reaction
SCD	standard chow diet
SEM	standard error of the mean
siRNA	small interfering RNA
SNP	sodium nitroprusside
TXA2	thromboxane A2
TXB2	thromboxane B2
VC	vacular calcification
VSMC	vascular smooth muscle cell

List of figures

List of tables

Abstract in German

Einleitung: Chronische Nierenerkrankungen (CKD) sind mit einer hohen kardiovaskulären Morbidität und Mortalität assoziiert. In der Pathogenese der CKD und den kardiovaskulären Folgeerkrankungen scheinen microRNAs (miRs) eine bedeutsame Rolle zu spielen. Daher haben wir den Zusammenhang zwischen miRs und endothelialer Dysfunktion bzw. urämischer Mediaverkalkung in der vorliegenden Arbeit näher untersucht.

Methoden: Wir untersuchten mittels qRT-PCR das Expressionsmusters von miRs in zwei unabhängigen Patientenkohorten mit chronischem Nierenversagen und validierten die dabei erhobenen Ergebnisse in einem Tiermodell mit urämischen DBA/2 Mäusen. In weiterer Folge wurden die funktionellen und morphologischen Auswirkungen der Behandlung von DBA/2 Mäusen mit miR-142-3p untersucht und zur Analyse ELISA, Western Blot, Massenspektrometrie und Myographie herangezogen.

Resultate: Patienten mit terminaler Niereninsuffizienz wiesen ein reguliertes Genexpressionsmuster von miRs auf, welche nach Nierentransplantation reversibel waren. Da miR-142-3p mit der carotid-femoralen Pulswellengeschwindigkeit in CKD 5D Patienten negativ assoziiert war, testeten wir die funktionellen und morphologischen Auswirkungen einer therapeutischen Substitution von miR-142-3p im Tiermodell. Dabei konnten wir zeigen dass die Acetylcholin-abhängige Relaxation der Aorta durch Behandlung mit synthetischem miR-142-3p deutlich verbessert werden konnte.

Fazit: Unsere Daten unterstreichen das therapeutische Potential von miR-142-3p gegen endotheliale Dysfunktion und arterielle Gefäßsteifigkeit in der terminalen Niereninsuffizienz (1).

Abstract in English

Introduction: Chronic kidney disease (CKD) is tightly associated with an increased risk of cardiovascular morbidity and mortality. There is also emerging evidence that different microRNAs (miRs) play relevant roles in the pathogenesis of CKD and the consequent vascular disease. The aim of this study was to investigate the potential role of microRNAs in uremic vascular disease and in the process of endothelial-mediated remodelling.

Methods: Using real time quantitative polymerase chain reaction we examined the expression profile of several microRNAS in two independent chronic kidney disease cohorts and in a mouse model of uremic media calcification. Furthermore, we treated the mice with an intravenous injection of synthetic miR-142-3p mimic in order to restore the bioavailability of the microRNA. Later the mice were evaluated for functional and morphological vascular changes by Western blot, mass spectrometry, ELISA, histology and wire myography.

Results: We found that several of the investigated microRNAs were regulated in our cohorts and in case of numerous microRNAS this regulation was reversible after kidney transplatation. We tested 19 microRNAs in our study and found that only miR-142-3p is negatively associated with carotid-femoral pulsewave velocity in CKD 5D patients. In our uremic mouse model of DBA/2 mice the same expression changes were found and the acetylcholine-mediated vascular relaxation of the aorta was also impaired in these animals, so we restored the bioavailability of microRNA-142-3p by injecting the synthetic miR-142-3p mimic. This injection improved the acetylcholine-mediated vascular relaxation of the aorta.

Conclusion: In this study, we present convincing evidence that microRNA-142-3p plays a role in uremic endothelial vascular dysfunction and could act as a potential pharmacological target in the treatment of end-stage renal disease in order to ameliorate endotelial dysfunction and arterial stiffness (1).

Introduction

The work described in this thesis investigates the role of microRNAs in chronic kidney disease and in concomitant vascular dysfunction as potential biomarkers and therapeutical targets. The aim of the study was to determine whether blood microRNA levels correspond with their concentration in the vessels and whether restoring healthy microRNA levels would ameliorate the symptoms caused by chronic kidney disease. The relevance of this study is that chronic kidney disease affects an enormous part of the worlds population and so far only limited amount of information is available about the involvement of microRNAs in the disease.

Kidney disease

Kidney disease is defined as „an abnormality of kidney structure or function with implications for the health of an individual, which can occur abruptly, and may either resolve or become chronic" by the 2012 Kidney Disease: Improving Global Outcomes (KDIGO) Clinical Practice Guideline for the Evaluation and Management of CKD (2). There are several factors which could cause different types of kidney diseases and then lead to chronic kidney disease and renal failure.

The metabolic, hemodynamic and structural changes in diabetes mellitus lead to damaged glomeruli in the kidney which then leads to albuminuria (3-5). It has also been showed that cytokines play a role in the progression of the disease (6). Due to the microangiopathy in diabetes mellitus, hypoxic conditions further deteriorate the condition. Approximately 10% of patients with diabetic nephropathy will develop end-stage renal disease and diabetic nephropathy is the most common cause of chronic kidney disease (7-10).

Elevated blood pressure leads to arteriolosclerosis and then glomerular and tubular changes in the kidneys. If this condition persists, a condition called hypertensive nephropathy will develop with the symptoms of proteinuria and hematuria. Hypertensive nephropathy is one of the leading causes of chronic kidney disease and could lead to kidney failure (11, 12).

Mutations in the PKD1, PKD2 or in the PKD3 genes lead to polycystic kidney disease (PKD). The main symptoms of the disease are cysts in the kidneys, hematuria and hypertension. Autosomal dominant polycystic kidney disease (ADPKD) is the most common hereditary renal disease and approximately 50% of the patients develop end-stage renal disease (13-15).

It has been shown that long term or excessive use of nonsteroidal anti-inflammatory drugs (NSAID), especially phenacetin, aspirin and paracetamol can cause analgesic nephropathy (16). The symptoms of the disease include high blood pressure, anaemia, pyuria, proteinuria and they follow a history of excessive analgesic consumption. The symptoms usually develop after the consumption of approximately 2-3 kilogramms of analgesics. Ultimately this condition could lead to end-stage renal disease and renal failure (17-19).

There are several other conditions which may lead to chronic kidney disease and then renal failure: infections, nephrotoxic drugs, autoimmune diseases, heavy metal poisoning and renal artery stenosis (7, 10, 20-22).

Chronic kidney disease

Classification of chronic kidney disease

The conceptual model of chronic kidney disease includes risk factors, kidney damage, decreased glomerular filtration rate (GFR) and renal failure. It was developed by the National Kidney Foundation's Kidney Disease Quality Outcome Initiative in 2002 and it was adopted by the international consensus of Kidney Disease: Improving Global Outcomes (2, 23). The definition of chronic kidney disease is kidney damage or glomerular filtration rate lower than 60 ml / min / 1,73 m^2 for at least three months, regardless of the cause of the disease (20-22). The markers of chronic kidney disease are pathological abnormalities, urine abnormalities (e.g. albuminuria), blood abnormalities (e.g. renal tubular syndromes), imaging abnormalities (e.g. polycystic kidneys, hydronephrosis, small and echogenic kidneys) and history of kidney transplantation (23). Albuminuria and GFR are the best markers for determining the seriousness of the disease. Albuminuria is the earliest marker of kidney damage in the case of diabetes mellitus, glomerular disease and hypertension. Albuminuria means increased glomerular permeability, and higher levels are associated with

increased risk for kidney and cardiovascular disease aggravation. Furthermore, therapies which decrease albuminuria are correlated with attenuated kidney disease progression (23). Generally, GFR is considered to be the best marker for kidney function in healthy individuals and in kidney disease patients. Clinically it is usually estimated from the serum creatinine levels (23). Due to the critical importance of kidney function in chronic kidney disease, the stages of the disease are determined by the GFR levels of the patients: stage 1 with GFR ≥ 90 ml / min / 1,73 m^2, stage 2 with GFR 60 – 89 ml / min / 1,73 m^2, stage 3 with GFR 30 – 59 ml / min / 1,73 m^2, stage 4 with GFR 15 – 29 ml / min / 1,73 m^2, stage 5 with GFR < 15 ml / min / 1,73 m^2 or the patient receives dialysis treatment (23). An improved system was introduced in 2012 by the Kidney Disease: Improving Global Outcomes Clinical Practice Guideline by combining GFR levels with albuminuria in order to define the stages of the disease, offer the best treatment strategies and to estimate the prognosis of the disease (2, 24). Six categories were developed based on GFR levels: G1 (normal or high): ≥90 ml / min / 1,73 m^2, G2 (mildly decreased): 60 – 89 ml / min / 1,73 m^2, G3a (mildly to moderately decreased): 45 – 59 ml / min / 1,73 m^2, G3b (moderately to severely decreased): 30 – 44 ml / min / 1,73 m^2, G4 (severely decreased): 15 – 29 ml / min / 1,73 m^2 and G5 (kidney failure): <15 ml / min / 1,73 m^2 (24). Albuminuria was divided into three groups, using the albumin – creatinine ratio (ACR): A1 (normal to mildly increased): < 30 mg / g, A2 (moderately increased): 20 – 300 mg / g and A3 (severely increased) > 300 mg / g (2, 24).

Prevalence and risk factors of chronic kidney disease

The prevalence of chronic kidney disease (stage 1-5) is 13,4% in the world and CKD stage 3-5 affects 10,6% of the population (25). Diabetes mellitus is the leading cause of chronic kidney disease and end-stage renal disease worldwide. The pathomechanisms which lead to the loss of kidney function include several molecular changes and 8% of the patients with diabetes mellitus type 2 have albuminuria (7, 8). Diabetes mellitus type 2 patients have an 11% 10-year risk of developing chronic kidney. Additionally, half of the type 2 diabetes mellitus patients will present symptoms of diabetic nephropathy and 10% of these patients will develop end-stage renale disease (7-10). Obesity is also a strong risk factor of developing ESRD. A body mass index higher than 30 kg / m^2 in men and higher than 35 kg / m^2 in women increases the risk of developing chronic kidney disease by 3 – 4 fold (26, 27). Arterial hypertension jointly with proteinuria is considered to be the most serious risk factor

in the progression of chronic kidney disease. Increased mean arterial pressure (MAP) leads to increased arterial pressure in the kidneys which will cause renal damage and glomerulosclerosis due to the repair mechanisms of the kidney (28, 29). Birth weight correlates with nephron numbers, thus low birth weight leads to an increased risk of developing chronic kidney disease. Decreased nephron numbers cause elevated blood pressure in the glomeruli, consequently leading to hyperfiltration in the nephrons and decreased glomerular filtration rate (30, 31). Additionally genetic factors are also a risk factor for chronic kidney disease. Almost 50% of the patients with polycystic kidney disease (PKD) develop ESRD until the age of 60 years (32). Acute kidney injury, age, ethnicity and gender also play roles in the development of chronic kidney disease (7, 32).

Complications of chronic kidney disease

Anemia is frequently diagnosed among patients with chronic kidney disease. Patients often develop iron deficiency due to dietary restrictions, deteriorating kidney function and adverse effects of medication. Many patients require iron treatment, usually in the form of infusion. Furthermore, the kidneys production of erythropoietin becomes deficient and the patients require supplemental therapy (33-35).

Pathogenic sodium retention in chronic kidney disease leads to hypertension, extracellular fluid volume expansion and can further facilitate the progression of the disease (36). It is important to maintain the extracellular fluid volume in the normal range in order to prevent progressive cardiovascular and kidney damage (37). Disturbed sodium balance and expanded extracellular fluid volume can lead to dyspnea, which is one of the most common symptoms associated with chronic kidney disease and can influence the patients quality of life to a great extent (38).

A frequent complication of chronic kidney disease is a disorder affecting the mineral and the bone metabolism, called chronic kidney disease – mineral and bone disorder (CKD-MBD). CKD-MBD is a systemic, clinical syndrome which is manifested by irregularities in bone and mineral metabolism and extraskeletal calcifications (39). CDK-MDB was defined as „a systemic disorder of mineral and bone metabolism due to CKD manifested by either one or a combination of the following: abnormalities of calcium, phosphorus, PTH, or vitamin D metabolism; abnormalities in bone turnover, mineralization, volume, linear growth, or

strength; vascular or other soft tissue calcification" by the KDIGO (39). There is increasing evidence that CKD-MBD is associated with increased risk for cardiovascular morbidity and mortality. The pathomechanism is not yet understood, but probably related to an effect on vascular calcification (VC) (40-43).

The high prevalence of vascular calcification is an important complication of chronic kidney disease. A casual, positive correlation has been proposed between the level of cardiovascular mortality and the extent of vascular calcification in chronic kidney disease. However, it is not yet clearly understood whether vascular calcification poses a risk itself or the underlying biological processes carry the additional risk (44). Vascular calcification is not a single entity, it can affect different layers of the vessels and it can be present at different anatomical locations (45-48). The calcification of the tunica intima is mainly caused by inflammation and depends on the migration of vascular smooth muscle cells and macrophages into the atheromatous lesion. Transdifferentiation into bone-forming cells is the primary mechanism of lesion calcification in the tunica intima (49). The other form of vascular calcification, the calcification of the tunica media is an active process and not just the deposition of calcium in the arterial wall. It is a response to different conditions affecting the arteries: aging, chronic kidney disease, inflammation and diabetes (50, 51). In patients receiving dialysis treatment, the progression and the prevalence of the disease increases quickly (52-54). The pathological mechanisms of tunica media calcification include local inflammation, phenotype switch of vascular smooth muscle cells and changed calcium and phosphate homeostasis (55). The phenotypic switch of vascular smooth muscle cells into osteoblast-like cells and the production of minerals are the key factors in tunica media calcification (56, 57). Both in media and intima calcification there are several factors which can modify the development and the progression of the condition, especially in chronic kidney disease patients. High serum phosphate levels deteriorate the disease while active vitamin-D can be protective against vascular calcification (58-61). Calcimimetics, vitamin-K and kidney transplantation are considered to be a treatment option for vascular calcification in chronic kidney disease as well (62-65). In conclusion, vascular calcification in chronic kidney disease is a complex pathological entity with different histological and pathophysiological properties which makes its prevention, diagnosis and treatment a complex task.

The primary cause of morbidity and mortality in chronic kidney disease is cardiovascular disease (CVD). CKD is an independent risk factor for cardiovascular events and it is an accelerator for cardiovascular risk. Chronic kidney disease (CKD) is tightly associated with an increased risk of cardiovascular morbidity and mortality (1, 66). The risk of cardiovascular disease and cardiovascular mortality is increased in end-stage renal disease (ESRD) patients 10-100-fold compared to patients with intact kidney function. This raise in risk can not be appropiately anticipated by the use of traditional risk factors (1, 67). Uremic media calcification, left ventricular hypertrophy, and sudden cardiac death are tightly correlated with the cardiovascular symptoms in chronic kidney disease and end-stage renal disease (1, 68, 69). Not only morphological cardiovascular changes are present in patients with chronic kidney disease, but reduced vascular compliance and an impairment of endothelium-dependent and endothelium-independent vascular function are also major factors in the development of the disease (1, 70, 71). Traditional risk factors only explain a minor section of cardiovascular disease in end-stage renal disease and conventional pharmacological therapies (e.g. statins) do not ameliorate the cardiovascular symptoms (72-74). It was previously described that uremic vascular dysfunction is shaped by several factors, including interruption of normal mineral and bone metabolism as well as uremic toxicty (1, 40, 75, 76). During uremic conditions, a diverse complex of regulators are responsible for the morphological and fuctional changes which lead to vascular calcification, transdifferentiation of vascular smooth muscle cells (VSMC), endothelial dysfunction and increased arterial stiffness. (1).

microRNAs

Definition and function of microRNAs

MicroRNAs (miRs) are small, non-coding RNA molecules, usually containing 22 nucleotides (77-79). The first microRNA was described in 1993, but their research only expanded after 2000 (80-84). Their main function is post-transcriptional modification of gene expression and RNA silencing (77-79). The potential therapeutic use of miRNAs is under investigation (85-88). MicroRNAs are part of the RNA-induced silencing complex (RISC), which also contains Dicer, Argonaute 2 (Ago2) and other proteins (89-92). MicroRNAs can silence their target by either mRNA degradation or by preventing the translation of the target mRNA (93-95).

MicroRNAs in diseases

Several microRNAs were associated with different diseases. miR2Disease is a database which collects known relationships between microRNAs and human diseases (96). So far, three mutations in microRNAs were identified as the cause of a genetic disease: mutation of miR-96 causes hereditary progressive hearing loss, mutation of miR-184 causes hereditary keratoconus with cataract and the mutation of miR-17 causes skeletal and growth defects (97-99).

Many microRNAs are associated with different cancers in humans. In non-small-cell lung carcinoma (NSCLC) low miR-324a levels correlate with worse survival outcomes (100). Low miR-133b or high miR-185 levels are associated with poor survival and higher risk of metastases in colorectal patients (101). miR-21, miR-494, and miR-1973 are biomarkers of Hodgkin lymphoma (102). MicroRNAs could be used as potential targets or drugs in different types of cancer (103).

MicroRNAs also play a role in the development of the nervous system and its proper function (104). MiR-132, miR-134, miR-138 and miR-124 take part in dendritogenesis, synapse formation and synapse maturation. MicroRNA expression was found to be altered in major depression, bipolar disorder and in schizophrenia (87, 105-108).

MicroRNAs also affect the differentiation of adipocytes (109, 110). miR-155, miR-221, and miR-222 are negative regulators of differentiation, whereas expression of these microRNAs inhibited adipogenesis (110, 111). The let-7 family of microRNAs play a role in the regulation of insulin resistance, obesity and diabetes. In mice, inhibition of the let-7 miR led to increased insulin sensitivity (112-114). These findings could open up therapeutic possibilities in the treatment of obesity and diabetes.

There is preliminary evidence that miRs play a role in the vascular smooth muscle cell phenotypic modulation and in the dysfunction of endothelial cells in uremia (75, 76, 115-118).

microRNA therapies

MicroRNAs play an important role in cell differentiation, survival and proliferation by regulating mRNA translation and they are disregulated in several diseases, mainly in cancer and cardiovascular diseases (78, 119-125). MicroRNAs are regularly affected in different diseases due to genomic events: mutations, deletions and transcriptional changes (78, 124, 126, 127). MicroRNAs provide excellent potential therapeutic solutions to several diseases because they can alter the expression of multiple dysregulated mRNA targets. Bioavailability of downregulated miRNAs could be restored by the use of microRNA mimics and endogenous microRNAs could be inhibited by antimiRs (122, 128-130). Furthermore, there is an emerging amount of delivery possibilities which make the therapeutic use of microRNAs feasible.

MicroRNA delivery methods

Viral vectors

MicroRNA coding adenoviruses can be constructed for research purposes, but this method has several limitations in the clinical practice, due to safety considerations (124, 131).

Poly(lactide-co-glycolide) particles

Poly(lactide-co-glycolide) (PLGA) is already used in the clinical practice as biodegradable sutures and it has low toxicity. Its effectiveness is limited by the fact that it has low affinity for siRNAs and miRNAs. The microRNA release can be regulated by changing the amount of nucleic acid bound to the PLGA particles (124, 132-134).

Neutral lipid emulsions, neutral liposomes

There are numerous lipid-based systems available for small interfering RNA (siRNA) and miRNA delivery. Neutral lipid emulsions are made of 1,2-dioleoyl-*sn*-glycero-3-phosphocholine (DOPC), their atomic charge is zero and they are not toxic. However, they have low penetration into cancer cells (124, 135). Nanoparticles made of DOPC are already used in preclinical studies and some of them reached phase I clinical trials (136-142).

TargomiRs

TargomiRs are bacterial particles of a size of approximately 400 nanometers. Their surface contains specific antibodies which makes it possible to target them to different cell types. An anti-epidermal growth factor receptor (EGFR) antibody coated nanoparticle is in phase I clinical trial, examining the efficiency of miR-16 mimic delivery (143, 144).

Synthetic polyethylenimine

Polyethylenimine (PEI) is one of the first nonviral delivery system for synthetic siRNAs and miRNAs (145). After binding to the selected miRNA, the complex keeps it positive charge, allowing it to bind to the negatively charged plasmamembrane. After endocytosis, the miRNAs can reach their targets in the cell. Polypus transfection SA (Illkirch-Graffenstaden, France) produces a commercially available jetPEI transfection reagent, which allows for in vivo transfection in mammals and is currently undergoing preclinical testing (1, 145).

Dendrimers

In dendrimers the nucleic acids (siRNA or miRNA) are conjugated to poly(propylenimine) or poly(amidoamine) polymers. These reagents have high effectiveness in animal experiments, however there are concerns about their toxicity (124, 146).

Cyclodextrin

Cyclodextrin is a glucose polymer and it is commonly used in pharmacological preparations. It has been used in clinical siRNA delivery trial and it showed significant effect on tumor cells. Due to its toxicity in higher doses the trial was cancelled (147, 148).

Poly(ethylene glycol)

In poly(ethylene glycol) (PEG) reagents the nucleic acid is conjugated by disulfide bonds. These molecules have high silencing efficiency which can be further increased by binding additional cyclodextrin molecules to the complex. There are clinical trials underway using these molecules (147, 149).

Chitosan

Chitosan is a cationic molecule which is produced from the polysaccharide chitin. It is widely used in preclinical research because of its low toxicity, biocompatibility and biodegradability. However, further research and modifications of this reagent are required in order to increase its effectiveness in in vivo studies (124, 150).

N-acetyl-D-galactosamine

N-acetyl-D-galactosamine (GalNAc) conjugated siRNAs and miRNAs get internalized by clathrin-mediated endocytosis. Some of these products are already in phase II clinical studies in order to investigate their effectiveness targeting hepatocytes. Due to their efficient elimanation by the liver, their effect on other organs are limited (151).

Application of microRNAs in clinical and preclinical studies

There are several phase I and phase II clinical studies investigating the effectiveness of microRNA therapies. The focus of these studies is mainly different types of cancer and liver diseases. AntimiR-122 is being tested in two studies for the treatment of hepatitis C. AntimiR-103/107 is investigated in a cohort of type 2 diabetes mellitus and non-alcoholic fatty liver disease. In a phase I trial a miR-16 mimic treatment is currently being investigated in mesothelioma and non-small cell lung cancer patients. The effects of a miR-34 mimic is being tested on several types of solid tumors (124).

Several studies are available about microRNA treatments in cardiovascular diseases in rodent models as well. MiR-21 is significantly upregulated in cardiac hypertrophy and fibrosis. Furthermore treatment with a synthethic miR-21 mimic causes apoptosis and fibrosis in a mouse pressure-overload-induced cardiac disease model (152). The miR-143/145 family is expressed in vascular smooth muscle cells and it is responsible for the regulation of several genes involved in proliferation and differentiation: ETS1, KLF4, KLF5, SSH2, SRGAP1, SRGAP2 and ACE. In mice, silencing of the miR-143/145 cluster cause hypertension and cardiac failure (153-156). MiR-1 plays a central role in the calcium signalling of myocytes through the regulation of calmodulin and the MEF2A transcription

factor. Silencing of miR-1 leads to fibrosis, hypertrophy and consequent heart failure in rats (157, 158). MiR-208 is also found in the heart and has a disadvantageous effect in cardiac stress. In a hypertensive model of Dahl rats, administering microRNA-208 mimics had a beneficial effect on cardiac function and hypertrophy (159, 160). MiR-33 downregulates several genes that play a role in atherosclerosis: ABCA1, CROT, CPT1A, AMPK, PCK1 and G6PC. Downregulation of these genes helps the progression of the disease. In primates kept on a high-fat diet, antimiR-33 treatment effectively increased the expression of the aforementioned genes and had no adverse effect on the animals after treating them for 10 weeks (161-163).

There is only a limited amount of data available about the role of microRNAs in vascular complications of chronic kidney disease. Furthermore, these experiments were carried out on apolipoprotein E knock-out mice, which is a model for atherosclerosis (164, 165). In order to study the role of microRNAs in uremic vascular calcification we designed clinical and experimental studies. We investigated the specific effects of microRNAs in vascular adaptation due to chronic kidney disease and the underlying mechanisms of vascular dysfunction. We also explored the possibility of using microRNAs as a pharmacological treatment in order to prevent harmful cardiovascular complications in end-stage kidney disease (1).

Materials and methods

Study population

We prospectively enrolled fifty-three consecutive hemodialysis (HD) patients at the Department of Dialysis of the University Clinical Centre Maribor, Slovenia, and nine consecutive peritoneal dialysis (PD) patients at the Clinical Division of Nephrology of the Medical University of Graz, Austria. The peritoneal dialysis patients were recruited immediately prior to kidney transplantation and controlled after one year. The eight Austrian healthy controls were matched for sex (63% male) and age (46.9±3.6 years). All of them had no relevant medical history, and did not take any regular medication. The study protocols were approved by the respective Institutional Review Boards of the University Clinical Centre Maribor (UKC-MB-KME-90/14) and the Medical University of Graz (25–207/ex 12/13), and complied with the Declaration of Helsinki. After obtaining written informed consent from the patients, peripheral blood was collected in PAXgene Blood RNA tubes (Qiagen, Venlo, Netherlands) and stored at -80 °C until evaluation.

Pulse wave velocity

Carotid-femoral pulse wave velocity (cfPWV) was performed in all hemodialysis patients in the morning between 8:00 and 11:00 under standardized conditions. Prior to the measurement, subjects were under similar conditions (abstained from coffee, cigarettes, heavy meals, and exercise). Each patient waited for 5–10 minutes in a quiet room before blood pressure recordings and cfPWV were taken. Before the cfPWV measurement office brachial diastolic and systolic blood pressure (BP) values have been obtained from a portable bedside monitoring automatic BP device (Dash 4000, General Electric Healthcare, Dallas, TX, USA). cfPWV was recorded using applanation tonometry (SphygmoCor, AtCor Medical, Ltd., Sydney, Australia). A single examiner performed all measurements. cfPWV was evaluated between the carotid and femoral artery with the participant lying in the supine position. Pulse measurements were performed non-invasively over the carotid and femoral artery while an ECG recording was performed simultaneously. A minimum of 12 seconds

of signal (approximately ten heartbeats) was recorded after a strong accurate and reproducible pulse wave signal was obtained. The distance from the carotid to femoral artery was measured directly between each artery location and the supra-sternal notch and the values were entered into the SphygmoCor software database. cfPWV was calculated by measuring the time delay between two characteristic timing points on two pressure waveforms that were at a known distance apart. The SphygmoCor method uses the foot of the waveform as an onset point for calculating the time differences between the R wave of the ECG and the pulse waveforms at each site. cfPWV was automatically calculated by the Atcor software as the carotid-femoral artery distance divided by the wave travelling time between the above 2 measuring sites. In each patient, a minimum of three cfPWV measurements were performed. The measurements with a standard deviation less than 10% were further evaluated and the average of these measurements were used for analysis. After the cfPWW measurement, ambulatory blood pressure monitoring was done for 48 hours using a Schiller BR-102 plus monitor (Schiller, Dietikon, Switzerland). Blood pressure was recorded every 20 minutes during the day and every 30 minutes during the night. The cuff of the blood pressure monitor was applied to the upper portion of the arm, and the patients were instructed to attend to their usual activities and medications.

Computed tomography

The computed tomography (CT) examinations of the heart and the pelvis were routinely performed on a Toshiba Aquilion 64-row detector CT scanner (Toshiba Medical Systems, Minato, Japan). The calcium score for coronary arteries, ascending thoracic, and infrarenal abdominal aorta was calculated by multiplying the calcification areas in mm^2 by a density score determined from the peak CT scan number (Agatston score) with a dedicated software (TeraRecon, Foster City, CA, USA) as previously described (1, 166).

Design of animal experiments

Female eight to ten week old dilute-brown agouti 2 (DBA/2NCrl, hereafter referred to as DBA/2) mice were obtained from Charles River (Sulzfeld, Germany) and housed in a virus/antibody-free environment. These mice have an inherent susceptibility to high-phosphate diettriggered calcification (167-169). To induce media calcification, they were placed on high-phosphate diet (HPD) from Altromin (Lage, Germany) containing 20.2 g phosphorus, 9.4 g calcium, 0.7 g magnesium, and 500 IU vitamin D3 per kg. The standard chow contained 7.0 g phosphorus, 10.0 g calcium, 2.2 g magnesium, and 1000 IU vitamin D3 per kg. Mice were then followed for 11 days and culled under anaesthesia. Female eight to ten weeks old C57BL/6J mice from Charles River were used in the same setup. All animal experiments were approved by the Austrian veterinary authorities (BMWF-66.010/0061-WF/V/ 3b/2016) and corresponded to the directive 2010/63/EU of the European Parliament. In a second set of experiments, female DBA/2 mice were again fed HPD for 11 days and then sacrificed under anaesthesia. On day 9, the mice were injected with the syn-mmu-miR-142-3p miR mimic (Qiagen, Venlo, Netherlands) or negative control siRNA (Qiagen) via the tail vein using the in vivo-JetPEI transfection reagent (Polypus transfection SA, Illkirch-Graffenstaden, France). Each mouse received 2 nmol syn-mmu-miR-142-3p miR mimic or 2 nmol Allstars Negative Control siRNA (Qiagen) as control with 4.28 µl in vivo-JetPEI transfection reagent in a final volume of 200 µl (1).

microRNA isolation, reverse transcription quantitative PCR

From mice, 100 µl peripheral blood was collected in RNAprotect Animal Blood Tubes (Qiagen), after which the tubes were incubated at room temperature for 3 hours and stored at -80 °C. Total RNA was isolated using the RNeasy Protect Animal Blood Kit (Qiagen), strictly following the manufacturer's instructions. Aortas from mice were stored in RNAlater (Sigma-Aldrich, St. Louis, MO, USA) at -80 °C and the mirVana miRNA Isolation Kit (Thermo Fisher Scientific, Waltham, MA, USA) was used to isolate RNA. Human blood samples in PAXgene Blood RNA Tubes were stored at -80 °C until evaluation. Total RNA was isolated using the PAXgene Blood miRNA kit (Qiagen, Venlo, Netherlands), strictly following the instructions of the protocol provided with the product. RNA was eluted in 40µl

Buffer BR5 and stored at -80°C. 200 ng total RNA was reverse transcribed with the miScript II RT Kit (Qiagen) using the miScript HiFlex Buffer. Real time quantitative PCR (RT-qPCR) was carried out on a CFX96 Real-Time PCR Detection System (Biorad, Hercules, CA, USA) using the miScript SYBR Green PCR kit (Qiagen) with the following miScript Primer Assays (Qiagen):

Hs_miR-21_2 Primer Assay (MS00009079)

,Hs_miR-21*_1Primer Assay (MS00009086)

Hs_miR-26b_1 Primer Assay (MS00003234)

Hs_miR-98_1 Primer Assay (MS00003367)

Hs_miR-98-3p_1 Primer Assay (MS00045136)

Hs_miR-103a_1 Primer Assay (MS00031241)

Hs_miR-125b_1 Primer Assay (MS00006629)

Hs_miR-142-3p_2 Primer Assay (MS00031451),

Hs_miR-145_1 Primer Assay (MS00003528)

Hs_miR-146a_1 Primer Assay (MS00003535)

Hs_miR-146a*_1 Primer Assay (MS00008715)

Hs_miR-155_2 Primer Assay (MS00031486)

Hs_miR-155*_1 Primer Assay (MS00008778)

Hs_miR-191_1 Primer Assay (MS00003682)

Hs_miR-210_1 Primer Assay (MS00003801)

Hs_miR-210-5p_1 Primer Assay (MS00045836)

Hs_miR-223_1 Primer Assay (MS00003871)

Hs_miR-223*_1 Primer Assay (MS00009184)

Hs_miR-423-5p_1 Primer Assay (MS00009681)

Hs_RNU6-2_11 Primer Assay (MS00033740)

2 ng reverse transcription product was used for each RT-qPCR reaction. RT-qPCR was evaluated using the ΔΔCq method. The miR expressions were normalized to the endogenous housekeeper RNU6b small nuclear RNA (1).

Biochemical analyses

From mice, 800-1000 µl blood was collected in Lithium Heparin (25 IU/ml blood) micro tubes (Sarstedt AG & Co., Nümbrecht, Germany) and centrifuged at 2000 g for 13 minutes, then the plasma was transferred to a new tube. Blood Urea Nitrogen (BUN) levels were measured using the SPOTCHEM EZ SP-4430 automated analyser (Arkray, Kyoto, Japan) with the appropriate test tubes and test strips (Menarini diagnostics, Vienna, Austria). Renal calcium content was determined using the Calcium Detection Assay Kit from Abcam (Cambridge, United Kingdom) following the manufacturer's instructions and normalized to the tissue weight (1).

Histology

After isolation, the kidneys of the mice were conserved for paraffin embedding in 4% formalin solution for 48 hours. Then the samples were paraffin embedded by an Automatic Tissue Processor (Leica, Wetzlar, Germany). Calcification was determined using 2% Alizarin Red S (Sigma-Aldrich) staining solution on 4 µm thick tissue sections. Kidney pathology was evaluated on periodic acid-Schiff (PAS) stained, 4 µm thick sections. The slides were evaluated, and pictures were taken with an Olympus BX43 light microscope and the cellSens Entry 1.14 program (Olympus, Shinjuku, Tokyo, Japan). PAS positive tubular casts were counted in 18 high power fields on 3 kidney sections per sample by two blinded and independent evaluators (1).

Mass spectrometry

Thoracic and abdominal aortas were isolated from the mice and stored at -80 °C until lyophilisation. The freeze-dried samples were weighed into 10 ml quartz tubes and 1 ml HNO_3 + 4 ml ultrapure water were added to each tube. The samples were placed into an Ultraclave III microwave heated autoclave (EMLS, Leutkirch, Germany). After pressurizing it with argon to 40 bar the following program was used to heat the samples: ramp in 10 minutes to 80°C, then in 15 minutes to 150°C, and in further 20 minutes to 250°C. This temperature was kept for 30 minutes. After cooling, the samples were transferred into 15 ml polypropylene tubes and diluted with ultrapure water to 10 ml. For quality control purposes bovine muscle reference material (RM8414, NIST, Gaithersburg, ML, USA) was digested with the samples. The concentrations of Ca, Mg and P with were determined with an inductively coupled plasma mass spectrometer (Agilent 7700x, Agilent, Waldbronn Germany). Therefore, external calibrations for the three elements were prepared in the concentration range from 10.0 µg/l up to 5000 µg/l. The nitric acid was adjusted to the digested solutions (10 % v/v HNO_3). The following isotopes were used for quantification: Ca (m/z=43), Mg (m/z=24) and P (m/z=31). The instrument was operated in the nogas mode. Be and Ge were added online as internal standards during the whole measurement (1).

Wire myography

Mouse aortic rings 2mm in length were isolated and positioned in small wire myograph chambers (Danish MyoTechnology, Aarhus, Denmark) containing physiological salt solution (PSS) (114 mM NaCl, 4.7 mM KCl, 0.8 mM KH2PO4, 1.2 mM MgCl2, 2.5 mM CaCl2, 25 mM NaHCO3 and 11 mM D-glucose, pH 7.4). PSS containing 60mM KCl (KPSS) was used to determine maximum contractility of the vessels. The rings were precontracted with increasing concentrations of norepinephrine (NE) (1nM-1µM), followed by endothelium-dependent relaxation to cumulatively increasing concentrations of acetylcholine chloride (ACh) (1nM-10µM). The endothelium-independent relaxation was examined by exposure of the rings to increasing concentrations of sodium nitroprusside (SNP) (1nM-1µM), a nitric oxide (NO) donor. Relaxation values were expressed as a percentage of the initial NE-induced contraction. To examine the involvement of

prostanoids, 10 μM diclofenac was added to the PSS during the myography procedure. The NO bioavailability was estimated from the constriction response to eNOS inhibitor Nω-nitro-L-arginine (L-NNA, 300 μM) in aortic rings precontracted with norepinephrine to 10% of the maximal contraction (1, 170-172).

Thromboxane and prostacyclin release from aortic rings ex vivo

Aortic rings were placed in separate wells of a 96-well plate in 150 μl DMEM (Sigma-Aldrich) supplemented with 10% FCS (Sigma-Aldrich) for 1 h under cell culture conditions (37 °C, 5% CO_2). The rings were then washed and stimulated with 10 μM ACh in DMEM without FCS for 10 min. After the stimulation the supernatants were collected. Thromboxane B2 (TXB2) was measured by a Thromboxane B2 Parameter Assay Kit (R&D Systems, Minneapolis, MN, USA), and 6-keto-$PGF_{1\alpha}$ was measured by the 6-keto-PGF_1 alpha ELISA Kit (Abcam, Cambridge, United Kingdom) from the supernatants strictly following the manufacturers' instructions (1).

Western blot

Aortas from control and mimic treated mice were isolated after 11 days of high phosphate diet and cut into 2mm rings. Subsequently, rings were put into 24 well dishes with 150 μl DMEM (Sigma-Aldrich) with 10% FCS (Sigma-Aldrich) for 1h under cell culture conditions (37 °C, 5% CO_2). Afterwards rings were treated with 10 μM acetylcholine (ACh) (Sigma-Aldrich) in DMEM without FCS at 37 °C for 10 min. After the treatment, rings were washed once with cold PBS and stored at -80 °C. Rings were homogenized in 200 μL RIPA Lysis and Extraction Buffer (Thermo Fisher Scientific) supplemented with 1 μL Protease Inhibitor Cocktail (Sigma-Aldrich) and 3 μL sodium orthovanadate (Merck, Darmstadt, Germany), a phosphatase inhibitor. After gel electrophoresis using 10% SDS-polyacrylamide gels for 90 minutes at 175 V, proteins were transferred to PVDF membrane for 90 minutes at 150 mA. PeqGOLD protein Marker IV (Peqlab, Radnor, PA, USA) was used as standard. After blocking in 5% BSA (Sigma-Aldrich), proteins were incubated with specific antibodies for total eNOS (BD Transduction Laboratories, Franklin Lakes, NJ, USA) phosphorylated

eNOS (pS1177; pT495) (BD Transduction Laboratories) and GAPDH (Cell Signaling Technology, Danvers, MA, USA), followed by appropriate HRP-conjugated secondary antibodies (Dako, Santa Clara, CA, USA). Protein signals were visualized by incubation with Millipore Western Blotting Substrate (Millipore Corporation, Billerica, USA) using a ChemiDoc system (Bio-Rad Laboratories, Vienna, Austria). Densitometric analyses were performed using the Image Lab software (Bio Rad) (1, 172).

Hemogram

800-1000 µl blood was collected in K3 EDTA (1,6mg/ml blood) micro tubes (Sarstedt AG & Co., Nümbrecht, Germany) and the differential hemograms were prepared by loading fresh whole blood into the V-Sight veterinary hematology analyzer from A. Menarini diagnostics (Vienna, Austria).

Statistical analysis

Data are presented as mean ± SEM or as median (with 25th and 75th percentile). Normal distribution of the data was assessed by the Kolmogorov-Smirnov test with Lilliefors correction. Linear regression analyses were performed to assess the association between blood miR levels and functional and morphological cardiovascular parameters, such as the carotid-femoral pulse wave velocity and calcium scores of the coronary arteries as well as the thoracic and abdominal aorta within the Slovenian cohort of CKD 5D patients. In addition to univariable analyses, we also adjusted for age, dialysis vintage, and insulin therapy, which are known confounders of vascular calcification and arterial stiffness. Differences between DBA/2 treatment groups were compared by either the non-parametric Mann-Whitney *U* test or the unpaired Student's t-test as appropriate depending on the distribution of the tested variable. The significance level was set to 5%. The statistical analyses were performed using GraphPad Prism 7.0 (GraphPad, La Jolla, CA) and R version 3.3.3 (1).

Results

miR-142-3p is associated with pulse-wave velocity in ESRD patients

The expression pattern of 19 blood miRs were investigated in this study. These microRNAs might have a role in chronic kidney disease, affecting vascular remodelling and endothelial dysfunction in patients. A conserved microRNA expression pattern was found in two independent chronic kindey disease stage 5 cohorts (Figure 1. and Table 1). The biochemical and clinical characteristics of this two cohorts are shown in Table 2. The investigated microRNA profile was independent of the type of dialysis (hemodialysis vs. peritoneal dialysis), age and dialysis vintage, and was reversible after kidney transplantation, as shown by the subgroup of Austrian patients who were followed-up one year after kidney transplantation (Figure 1. and Table 1.), indicating that it might be an early event in the pathological reaction to uremia. The association between the investigated microRNA levels and morphological or functional cardiovascular parameters were assessed by linear regression analyses in the Slovenian cohort (fifty-three CKD 5D patients). Pulsewave velocity and calcium score were used as dependent variables for this purpose. Only miR-142-3p displayed a significant negative association with the carotid-femoral pulse wave velocity ($p = 0.025$) from the investigated nineteen microRNAs (Table 3.). Surprisingly, there was no significant association of blood miR-142-3p with calcium scores of the coronary arteries, thoracic or abdominal aorta. None of the other analysed microRNAs showed significant correlation with calciun scores of these vessels neither. After adjusting the univariable models for insulin therapy, age and dialysis vintage, there was still a trend for an association of miR-142-3p with carotid-femoral pulse wave velocity ($p = 0.062$) (1).

In order to validate the results of this bicentric, observational study and to provide an animal model for investigating microRNAs in chronic kidney disease, the same microRNA expression panel was measured in a murine CKD model and respective murine controls. DBA/2 and C57BL/6 mice were used for this purpose and they were fed high-phosphate diet in order to induce kidney calcification and concomitant chronic kidney disease. DBA/2 mice carry a splice variant of the ATP-binding cassette sub-family C member 6 (*Abcc6)* gene which encodes an anion transporter. Due to their different genetic background, they develop a phosphate-induced nephropathy, whereas C57BL/6 mice do not show any renal phenotype when fed high-phosphate diet. DBA/2 mice develep uremia a few days after the start of high-

phosphate diet and they quickly reach end-stage renal disease. After eleven days of high-phosphate diet, peripheral blood was collected from the mice and the expression of the microRNA panel was measured via RT-qPCR. DBA/2 mice had apparent phosphate-induced nephropathy after eleven days and we found similar microRNA expression patterns in the blood of uremic DBA/2 mice and in the blood of end-stage renal disease patients (Figure 1. and Table 1.). Furthermore, the same microRNA expression pattern was seen in the aortic tissue of DBA/2 mice after eleven days of high-phosphate diet (Figure 1.). C57BL/6 mice after eleven days of high-phosphate diet had no kidney disease and showed the same microRNA expression pattern as C57BL/6 mice on standard chow (Table 1. and Figure 2.) These findings show that the regulation of microRNAs was not directly induced by the high-phosphate diet (1).

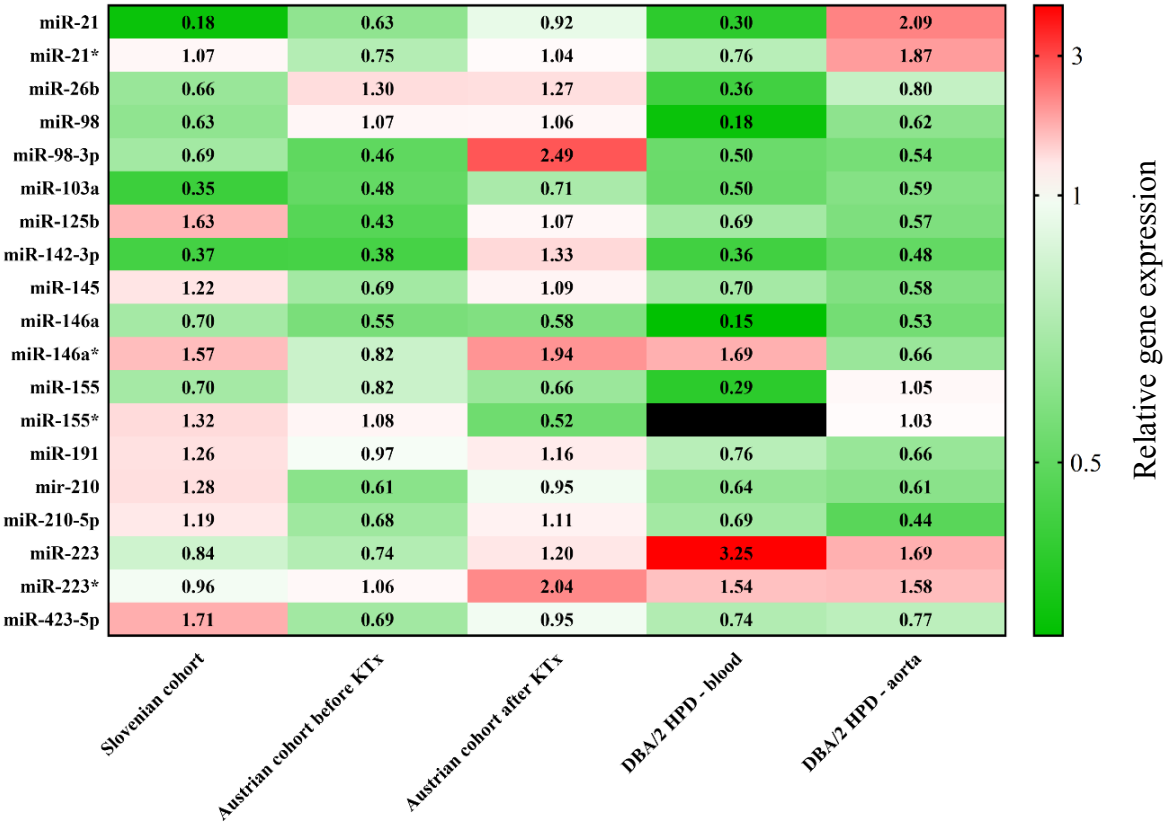

Figure 1.

Conserved miR expression patterns in mice and patients with uremia

Expression of nineteen microRNAs was analysed by quantitative RT-PCR in the peripheral blood of two independent chronic kidney disease 5D cohorts and a subset of patients after kidney transplantation (KTx) (n = 3). The data was normalized to healthy controls and the mean relative fold change is given in green for downregulation and in red for upregulation, respectively. Moreover, expression of the same panel was examined in the blood and aorta of uremic DBA/2 mice and normalized to healthy controls. Data shown in this figure was previously published (1).

	Slovenian cohort [a]	Austrian cohort before KTx [a]	Austrian cohort after KTx [a]	DBA/2 [b]	C57BL/6 [c]
miR-21	0.18 ± 0.14 ***	0.63 ± 0.65	0.92 ± 0.59	0.30 ± 0.11	1.00 ± 0.49
miR-21*	1.07 ± 1.17	0.75 ± 0.26 *	1.04 ± 0.22	0.76 ± 0.17	0.99 ± 0.41
miR-26b	0.66 ± 0.45 *	1.30 ± 1.11	1.27 ± 0.53	0.36 ± 0.07 *	0.98 ± 0.29
miR-98	0.63 ± 0.62 *	1.07 ±1.00	1.06 ± 0.69	0.18 ± 0.06 **	1.11 ± 0.4
miR-98-3p	0.69 ± 0.81	0.46 ± 0.29 *	2.49 ± 0.44 *	0.50 ± 0.16	1.98 ± 0.84
miR-103a	0.35 ± 0.32 ***	0.48 ± 0.44 *	0.71 ± 0.16	0.50 ± 0.16	1.00 ± 0.36
miR-125b	1.63 ± 1.96	0.43 ± 0.34 *	1.07 ± 0.63	0.69 ± 0.22	1.02 ± 0.44
miR-142-3p	0.37 ± 0.28***	0.38 ± 0.24*	1.33 ± 0.26	0.36 ± 0.14***	1.12 ± 0.46
miR-145	1.22 ± .1.21	0.69 ± 0.22 *	1.09 ± 0.54	0.70 ± 0.2	1.23 ± 0.39
miR-146a	0.70 ± 0.55 *	0.55 ± 0.39 *	0.58 ± 0.31	0.15 ± 0.09 **	1.00 ± 0.27
miR-146a*	1.57 ± 2.06	0.82 ± 0.73	1.94 ± 0.81	1.69 ± 0.92	2.20 ± 0.47 *
miR-155	0.70 ± 0.67	0.82 ± 0.73	0.66 ± 0.33	0.29 ± 0.08 **	1.07 ± 0.29
miR-155*	1.32 ± 1.33	1.08 ± 0.48	0.52 ± 0.55		
miR-191	1.26 ± 1.45	0.97 ± 0.13	1.16 ± 0.32	0.76 ± 0.17	0.99 ± 0.41
mir-210	1.28 ± 1.56	0.61 ± 0.26 *	0.95 ± 0.09	0.64 ± 0.15*	0.99 ± 0.33
miR-210-5p	1.19 ± 1.62	0.68 ± 0.17 **	1.11 ± 0.23	0.69 ± 0.1 *	1.10 ± 0.4
miR-223	0.84 ± 0.62	0.74 ± 0.48	1.20 ± 0.09	3.25 ± 0.72 ***	1.05 ± 0.48
miR-223*	0.96 ± 1.1	1.06 ± 0.33	2.04 ± 0.76 **	1.54 ± 0.42	1.00 ± 0.29
miR-423-5p	1.71 ± 2.4	0.69 ± 0.23 *	0.95 ± 0.19	0.74 ± 0.21	1.10 ± 0.37

Table 1.

miR expression patterns in mice and patients with chronic kidney disease

[a] Relative gene expression compared to healthy controls

[b] Relative gene expression compared to DBA/2 mice on standard chow diet

[c] Relative gene expression compared to C57BL/6 mice on standard chow diet

Multiple comparisons with Bonferroni-Dunn correction.

KTx = Kidney transplantation.

* indicates $p \leq 0.05$, ** $p \leq 0.01$, and *** $p \leq 0.001$.

Data shown in this table was previously published (1).

	Slovenian CKD G5D cohort	Austrian CKD G5D cohort	
	n=53	Before KTx (n=9)	After KTx (n=3)
Gender (male; %)	68%	67%	100%
Age (years)	63.1 ± 2.0	44.9 ± 4.0	43.3 ± 7.3
Dialysis vintage (months)	61.7 ± 7.9	43.8 ± 8.4	37.0 ± 11.9
Hemodialysis (%)	100%	0%	0%
Peritoneal dialysis (%)	0%	100%	0%
Leukocytes (G/L)	6.0 ± 0.3	6.8 ± 0.6	7.2 ± 2.0
Hemoglobin (g/L)	112 ± 1	113 ± 6	134 ± 10
Calcium (mmol/L)	2.14 ± 0.03	2.19 ± 0.07	2.44 ± 0.04
Phosphate (mmol/L)	1.62 ± 0.05	1.62 ± 0.09	0.97 ± 0.13
Magnesium (mmol/L)	1.22 ± 0.18	1.01 ± 0.08	0.74 ± 0.04
C-reactive protein (mg/dL)	6.2 ± 0.9	2.6 ± 1.2	2.2 ± 1.4
Parathyroid hormone (ng/L)	287.1 ± 22.6	291.2 ± 48.6	142.9 ± 26.4
Creatinine (mg/dL)	9.59 ± 0.24	9.04 ± 0.99	1.67 ± 0.24
BUN (mg/dL)	134 ± 3	119 ± 9	66 ± 13
Systolic blood pressure (mmHg)	138 ± 2	132 ± 5	125 ± 3
Diastolic blood pressure (mm Hg)	75 ± 2	85 ± 4	82 ± 2
Coumarin (%)	0%	22%	33%
Sevelamer (%)	69%	100%	0%
Cinacalcet (%)	21%	22%	0%
Calcitriol (%)	51%	44%	0%
Lanthanum carbonate (%)	6%	0%	0%
Statin (%)	31%	33%	0%
Insulin (%)	31%	0%	33%
Coronary calcium score	914 (52, 1767)	139 (12, 179)	
Ca score of the ascending aorta	84 (0, 819)		
Ca score of the abdominal aorta	5655 (1356, 9990)		
Pulse wave velocity (m/s)	11.27 ± 0.43		

Table 2.

Clinical and biochemical characteristics of patient cohorts with CKD

Data shown in this table was previously published (1).

	Pulse wave velocity			Calcium score		
	estimate	lower-upper CI	p-value	estimate	lower-upper CI	p-value
miR 21	4.93	-0.87-10.73	0.094	-0.48	-14.34-13.39	0.945
miR-142-3p	2.87	0.38-5.36	0.025	-0.34	-6.47-5.79	0.912
miR-155	0.68	-1.44- 2.80	0.524	-0.97	-5.98-4.04	0.698
miR-98	1.81	-0.63-4.24	0.143	0.01	-5.76-5.79	0.996
miR-98-3p	0.02	-3.25-3.29	0.991	-2.74	-10.42-4.95	0.478
miR-125-b	0.09	-0.55-0.73	0.776	-0.07	-1.56-1.42	0.926
miR145	0.00	-1.51-1.50	0.998	-2.56	-6.18-1.05	0.161
miR146a	0.68	-0.48-1.85	0.245	-0.11	-2.86-2.64	0.937
miR-210	0.18	-0.97-1.33	0.756	-0.78	-3.46-1.89	0.559
miR210-5p	-0.33	-2.08-1.42	0.706	-1.59	-5.86-2.68	0.457
miR-223	0.55	-0.81-1.92	0.419	-1.61	-4.87-1.65	0.326
miR-223*	0.72	-1.03-2.47	0.413	-0.34	-4.46-3.78	0.869
miR-423-5p	-0.70	-1.80-0.41	0.212	-0.68	-3.29-1.93	0.603
miR-21*	0.12	-1.53-1.77	0.886	-0.69	-4.57-3.19	0.722
miR-26b	0.01	-2.01-2.03	0.991	-2.88	-7.51-1.74	0.216
miR-103a	0.34	-3.03-3.71	0.839	-3.81	-11.56-3.93	0.327
miR-145*	-0.11	-1.31-1.09	0.852	-1.15	-3.98-1.69	0.420
miR-146*	0.55	-0.01-1.12	0.053	0.76	-0.58-2.09	0.258
miR-155*	0.26	-1.39-1.90	0.757	0.78	-3.10-4.65	0.689
miR-191	-1.51	-3.26-0.24	0.089	-2.10	-6.38-2.18	0.328

Table 3.

Linear regression analysis of blood microRNAs

Linear regression analyses of blood microRNA levels with carotid-fermoral pulse wave velocity and aortic calcium score in 53 ESRD patients. Data shown in this table was previously published (1).

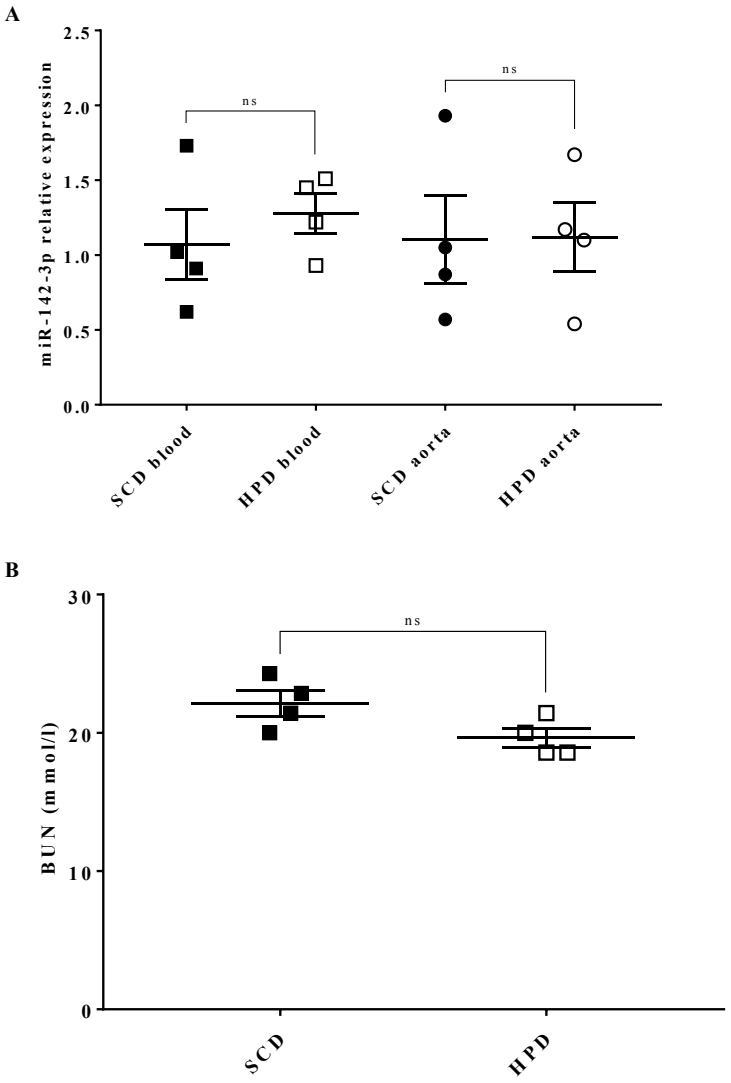

Figure 2.

High phosphate diet per se did not regulate miR-142-3p expression in C57Bl/6 mice

(**A**) The expression of miR-142-3p was evaluated by qRT-PCR in the blood (squares) and aorta (circles) of C57BL/6 mice after 11 days of standard chow (SCD) (closed symbols) or high-phosphate diet (HPD) (open symbols). (**B**) Blood urea nitrogen (BUN) was not elevated in C57Bl/6 mice exposed to HPD for 11 days (n=4, open squares) when compared to controls on SCD (n=4, closed squares). Data shown in this figure was previously published (1).

Injection of syn-mmu-miR-142-3p restores miR-142-3p bioavailability

Since we only found a significant negative association between microRNA-142-3p and carotid-femoral pulse wave velocity, we specifically focused on this microRNA and its role in chronic kidney disease. In the investigated chronic kidney disease cohorts with dialysis treatment, blood microRNA-142-3p levels were significantly lower than in the healthy control group (Figure 3.). Three patients already underwent kidney transplantation in the Austrian cohort and their microRNA-142-3p blood levels were similar to the healthy controls (Figure 3.). DBA/2 mice showed a similar downregulation of blood microRNA-142-3p after eleven days of high phosphate diet (Figure 3.). However, high-phosphate diet had no effect on the microRNA-142-3p expression in C57BL/6 mice after eleven days, excluding the possibility of a direct, diet induced effect (Figure 2.). In order to further investigate the functional consequences of the microRNA-142-3p downregulation in our model, we designed experiments to restore the bioavailability of microRNA-142-3p. We used the JetPEI delivery system with a synthetic microRNA mimic (syn-mmu-miR-142-3p) which was administered to the mice via tail vein injections. The mice were injected on the ninth day of high-phosphate diet, then sacrificed and evaluated on the eleventh day. With this intravenous experimental intervention, aortic miRNA-142-3p bioavailability was successfully restored in our animal model (Figure 3.). Furthermore, the syn-mmu-miR-142-3p treatment had no effect on kidney function or morphology. There was no diffrence between the syn-mmu-miR-142-3p and the control treated mice on high phosphate diet in regards of renal calcification and PAS positive tubular casts. Kidney function was also similar between the high-phosphate fed groups after eleven days of high-phosphate diet, which was estimated by blood urea nitrogen levels. Compared to standard chow fed mice, both high-phosphate diet fed groups had higher PAS scores, increased renal calcification and elevated blood urea nitrogen levels (Figure 4.).

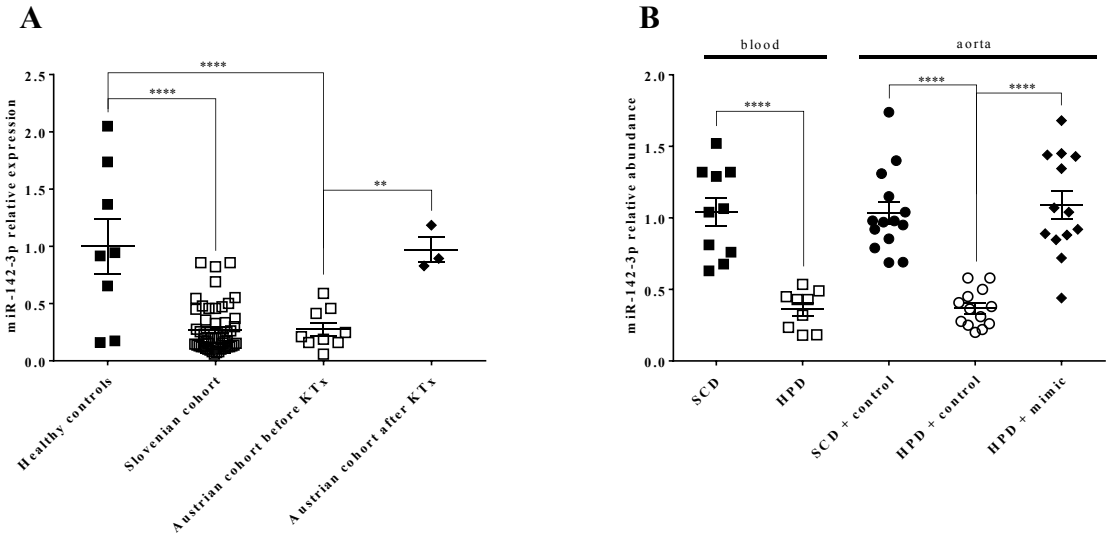

Figure 3.

miR-142-3p is downregulated in uremic patients and mice

(A) miR-142-3p expression was analysed by quantitative RT-PCR in the blood of two independent CKD 5D cohorts (n = 53 and n = 9, open squares), and a subset of CKD patients after kidney transplantation (KTx) (n = 3, closed diamonds). The expression was normalized to healthy controls (n = 8, closed squares). (B) miR-142-3p expression was analysed in the blood of DBA/2 mice on high phosphate diet (HPD) (n = 10, open squares) and compared to controls on standard chow (SCD) (n = 9, closed squares). miR-142-3p relative abundance was also measured in murine aortas with control siRNA injection (n = 13, open circles) and compared to controls on SCD (n = 14, closed circles), and mice on HPD treated with syn-mmu-miR-142-3p (n = 13, closed diamonds). Data represent mean ± SEM. ** indicates $p < 0.01$;**** indicates $p < 0.0001$. Data shown in this figure was previously published (1).

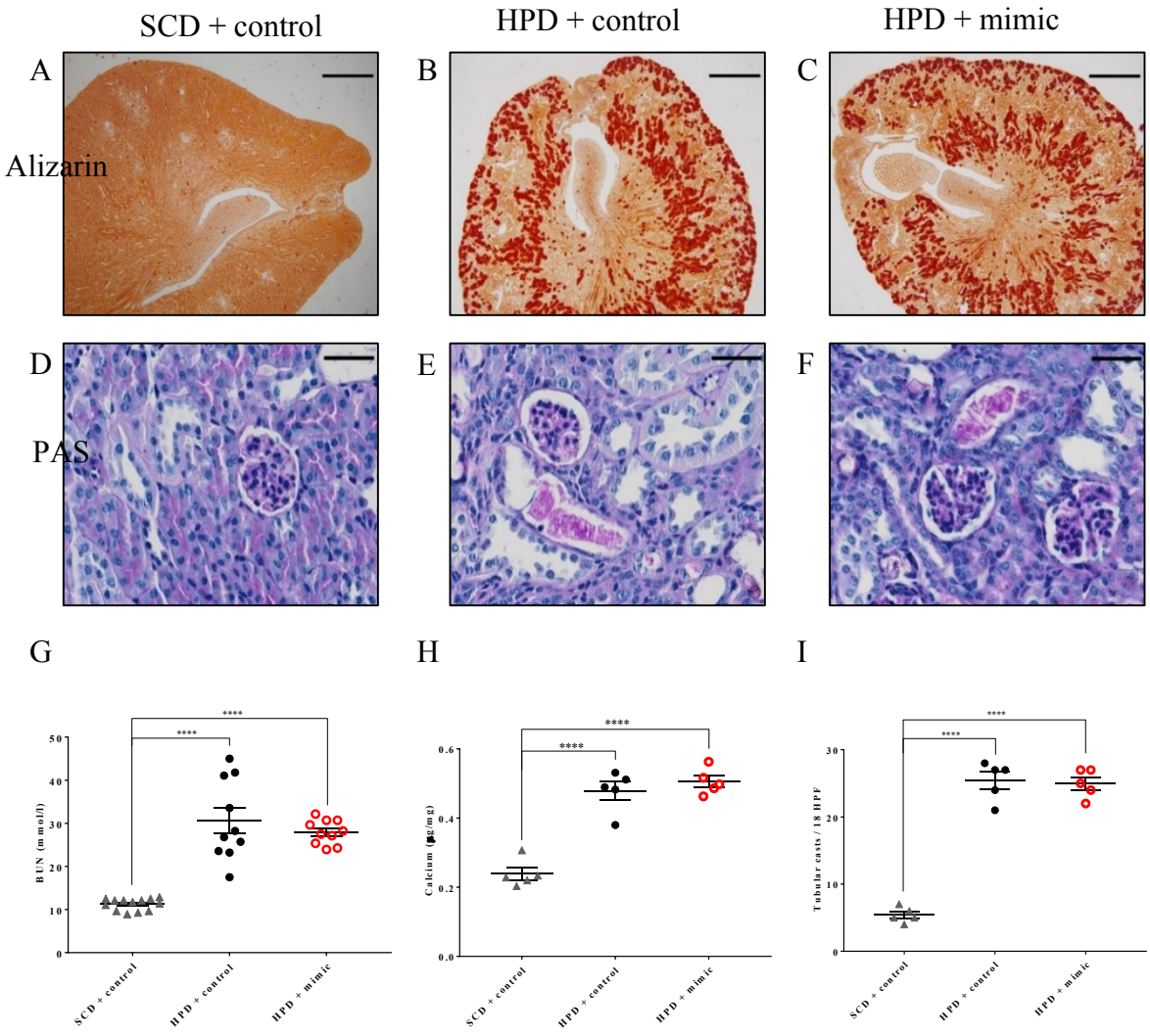

Figure 4.

Treatment with syn-mmu-miR-142-3p did not affect renal phenotype

DBA/2 mice were fed standard chow (SCD) or high-phosphate diet (HPD), and were treated with syn-mmu-miR-142-3p mimic or negative control siRNA 48 hours before the end of the experiment. The mice were divided into 3 treatment groups: SCD with control injection (A, D; grey triangles), HPD with control injection (B, E; closed circles), and HPD with mimic injection (C, F, red open circles). Renal calcification was detected by Alizarin Red S staining on kidney sections (A-C) and by measuring the total calcium content of kidneys (H). Tubular casts were counted in PAS stained kidney sections (D-F, I). Kidney function was assessed by blood urea nitrogen (BUN) levels (G). Representative images are shown (A-F). Data represent mean ± SEM. ****indicates $p < 0.0001$. The size bars display 500 μm for A-C and 25 μm for D-F. Data shown in this figure was previously published (1).

Syn-mmu-miR-142-3p improves aortic relaxation attenuated by uremia

In order to further analyse the specific role of microRNA-142-3p on vascular phenotype and to get more insight into the mechanisms involved, we designed exeriments and evaluated the mineral content of aortic rings by mass spectrometry. DBA/2 mice were fed high phosphate diet for eleven days and they were either injected with the syn-mmu-miR-142-3p microRNA mimic or a negative control two days before the end of the experiment. The aortas of the mice were isolated, lyophilised and evaluated by mass spectrometry. Despite the succesful restoration of microRNA-142-3p bioavailability, there were no significant differences in calcium, phosphorus and magnesium content between the treated and the control group (Figure 5.).

In another set of experiments, we used wire myography to measure functional parameters of explanted aortic rings. We found that uremia, caused by eleven days of high phosphate diet, significantly increased the KPSS-mediated contraction of the aortic rings, as well as their maximum contraction force. Uremia had no effect on norepinephrine-mediated contraction. These functional parameters were not affected by the syn-mmu-miR-142-3p treatment (Figure 6.).

Acetylcholine-induced relaxation was examined on norepinephrine-precontracted aortic rings. We observed an impaired relaxation in uremic mice compared to DBA/2 mice which were fed standard chow, but acetylcholine-induced relaxation was restored to control levels in mice treated with syn-mmu-miR-142-3p. Neither chronic kidney disease with uremia, nor restored microRNA-142-3p bioavailability had any effect on sodium nitroprusside-mediated relaxation (Figure 7.).

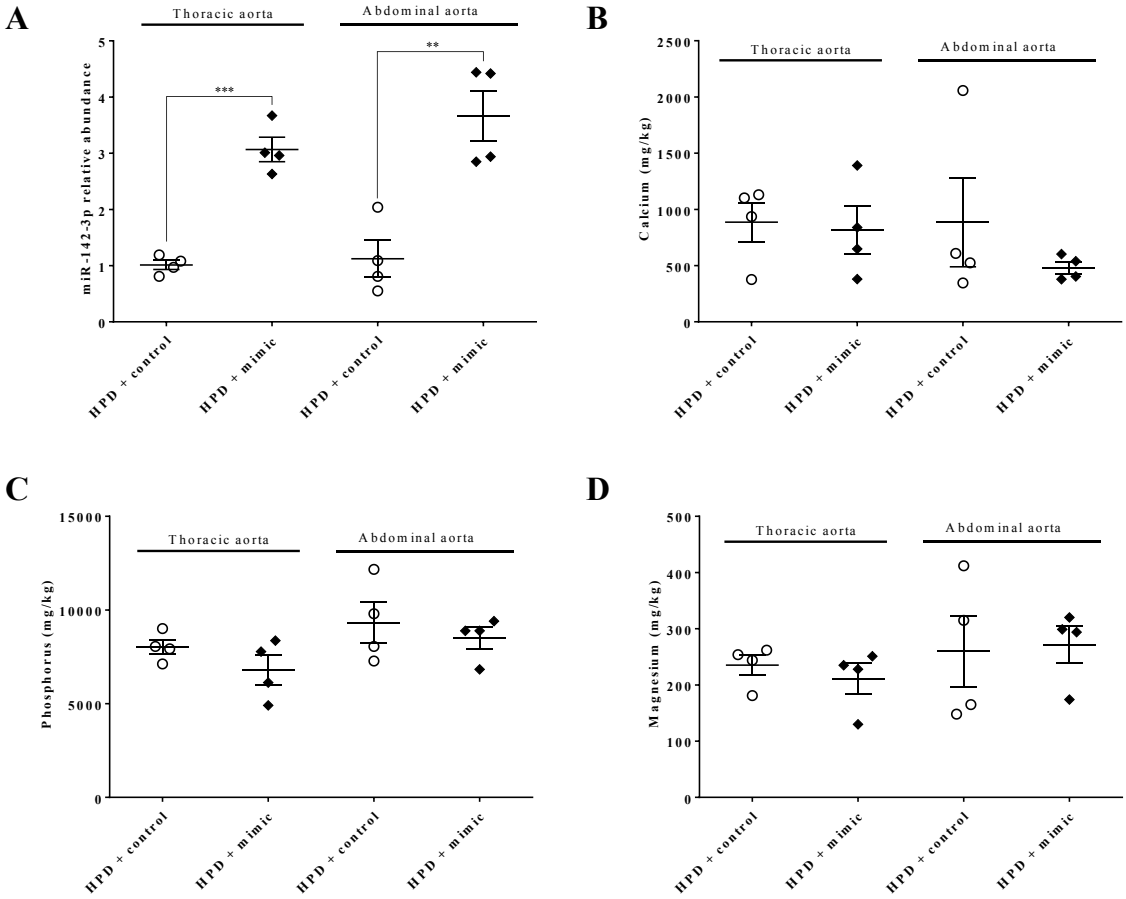

Figure 5.

Mineral deposition in DBA/2 mice after injection of syn-mmu-miR-142-3p mimic

Measurement of calcium (B) phosphorus (C) and magnesium (D) content in aortic tissue by mass spectrometry after succesful treatment of uremic DBA/2 mice with syn-mmu-miR-142-3p mimic and respective controls (A). Data shown in this figure was previously published (1).

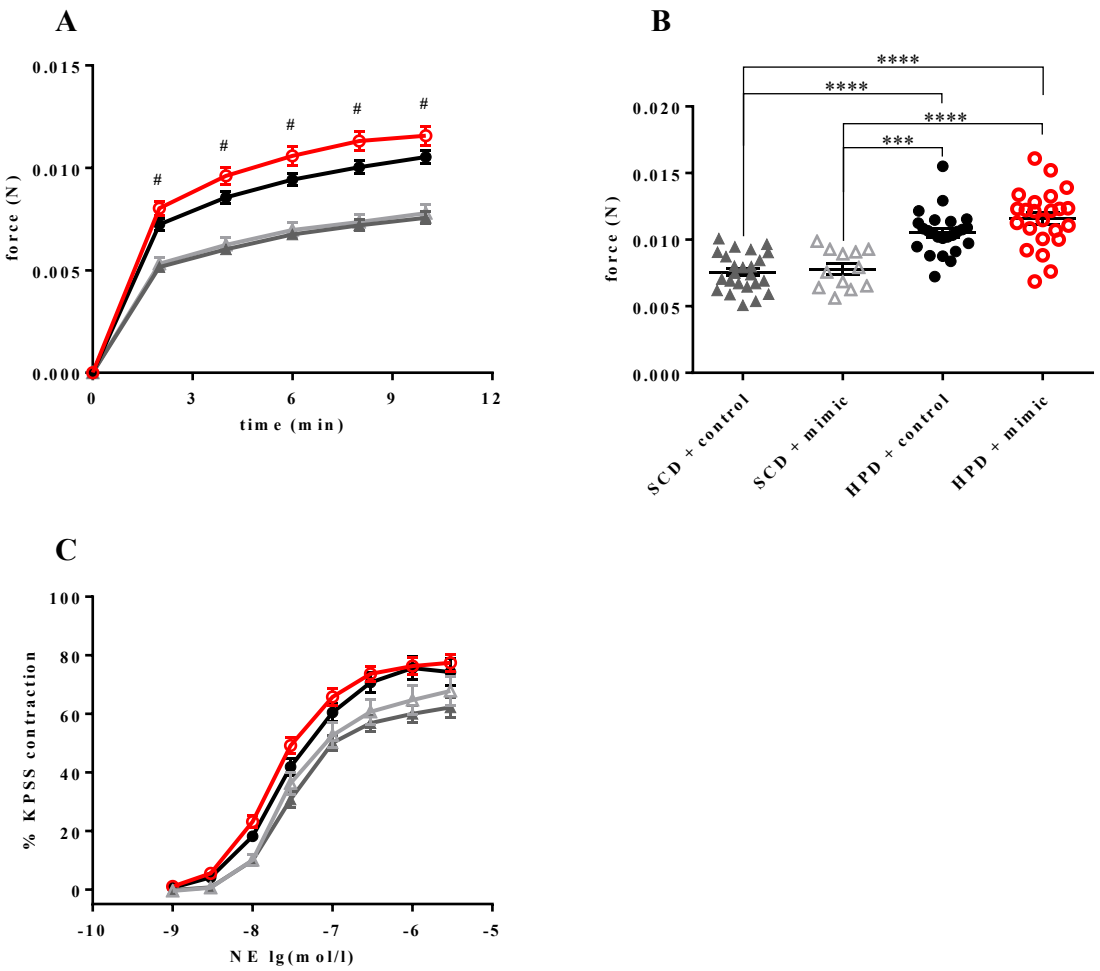

Figure 6.

Effects of high phosphate diet on aortic contraction

DBA/2 mice were either fed standard chow (SCD) or high-phosphate diet (HPD) and were treated with syn-mmu-miR-142-3p mimic or negative control siRNA 48 hours before the end of the experiment. Animals were divided into four treatment groups: SCD with control injection (grey closed triangles), SCD with mimic injection (grey open triangles), HPD with control injection (closed circles), and HPD with mimic injection (red open circles). KPSS contraction over time (A), maximum KPSS contraction force (B) and norepinephrine-induced contraction (C) were evaluated in all four groups. Data represent mean ± SEM. * indicates ***$p < 0.001$, and ****$p < 0.0001$ between mice on HPD that were treated either by injection of syn-mmu-miR-142-3p mimic or negative control siRNA. # indicates $p < 0.05$ between HPD + control and SCD + control groups. Data shown in this figure was previously published (1).

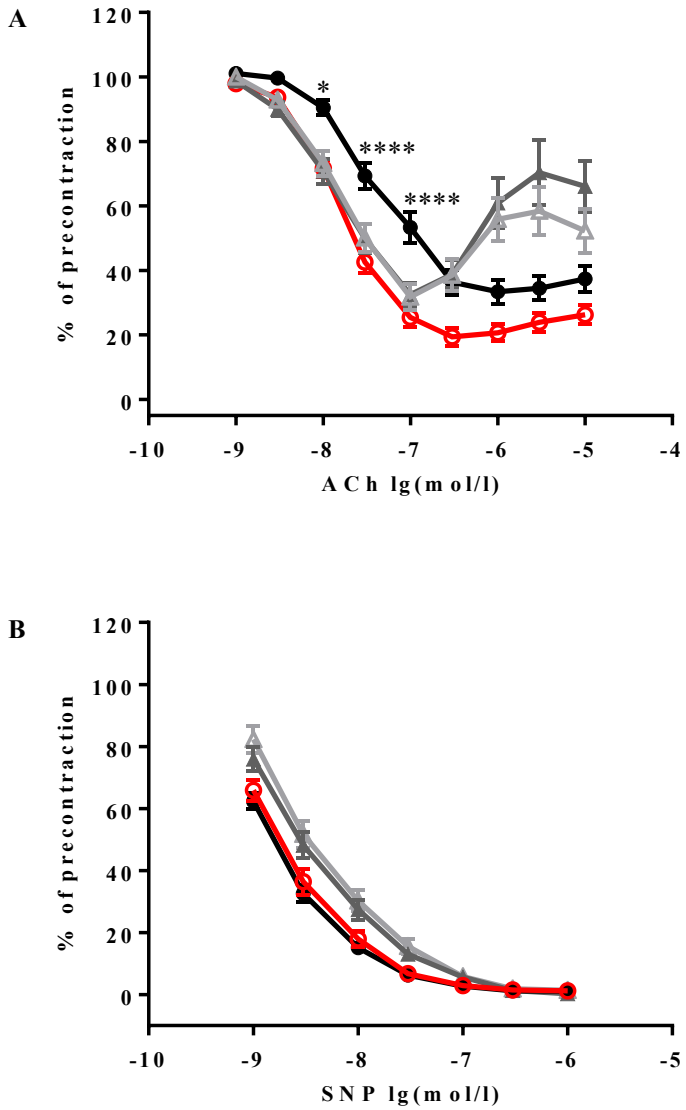

Figure 7.

Syn-mmu-miR-142-3p restores aortic relaxation attenuated by uremia

DBA/2 mice were either fed standard chow (SCD) or high-phosphate diet (HPD) and were treated with syn-mmu-miR-142-3p mimic or negative control siRNA 48 hours before the end of the experiment. Animals were divided into 4 treatment groups: SCD with control injection (grey closed triangles), SCD with mimic injection (grey open triangles), HPD with control injection (closed circles), and HPD with mimic injection (red open circles). Acetylcholine (ACh)-induced relaxation of NE-precontracted aortic rings (A) and sodium nitroprusside (SNP)-mediated relaxation of NE-precontracted aortic rings (B) were evaluated in all four treatment groups. Data represent mean ± SEM. * indicates *$p < 0.05$ and ****$p < 0.0001$ between mice on HPD that were treated either by injection of syn-mmu-miR-142-3p mimic or negative control siRNA. Data shown in this figure was previously published (1).

In order to identify the mechanisms contributing to the syn-mmu-miR-142-3p-mediated restoration of acetylcholine-induced relaxation of aortic rings from uremic mice, we investigated the role of endothelial-derived prostanoids in our model. For this purpose, after eleven days of high-phoshate diet, and two days after the sny-mmu-miR-142-3p mimic injection the DBA/2 mice were sacrificed and their aortas were isolated. The aortas were cut into 2 mm wide rings and treated with acetylcholine in standard cell culture plates. Then thormboxane B2 (TXB2) and 6-keto-$PGF_{1\alpha}$ were measured from the supernatants. We detected a significant down-regulation of the potent vasoconstrictor thromboxane A2 by measuring its metabolic product, thormboxane B2 (TXB2) in the supernatants when comparing syn-mmu-miR-142-3p treated mice to respective negative controls. Furthermore, the concentration of the vasodilatator prostacyclin (PGI2) was determined by measuring its metabolic product, 6-keto-$PGF_{1\alpha}$ from the same samples and showed no difference between the treatment groups (Figure 8.) (1).

Therefore, to further investigate the effect of prostanoids, myography was done in the presence of a cyclooxygenase inhibitor, diclofenac. As shown in Figure 9., diclofenac had no effect on the contraction of the vessels after KPSS or norepinephrine stimulation. Also, diclofenac did not fully abolish the effect of syn-mmu-miR-142-3p treatment on ACh-induced relaxation (Figure 10.). For this reason, in the same experimental setup, we assesed the dose-response curve of acetylcholine on vascular relaxation in the presence and in the absence of diclofenac on control and on syn-mmu-miR-142-3p treated aortic rings. The IC50 values were calculated via nonlinear regression curve fitting and were significantly different in all four groups ($p < 0.001$) (Figure 11.). These findings suggested that the contribution of syn-mmu-miR-142-3p-mediated changes of prostanoid synthesis play a significant role in the recovery of relaxation, but it is not solely responsible for the restoration of relaxation, additional mechanisms might be involved (1).

In order to further dissect the effects of miR-142-3p on endothelium-mediated vascular relaxation, we determined the protein levels of endothelial nitric oxide synthase (eNOS) and its phosphorilated forms (peNOS) from the aortas by Wester blot analyses. The mimic treatment had no effect on eNOS protein expression and it did not change Ser1177 activating or Tyr495 inhibitory phospharilation (Figure 12.).

Furthermore, the basal nitric-oxide bioavailability was assessed on explanted, NE-preconstricted aortic rings. The L-NNA-induced endothelium-dependent constrictor response, indicative of basal NO bioavailability, was significantly decreased in the aortic rings of mice with uremia compared to the control, standard chow fed mice. Syn-mmu-miR-142-3p injection did not restore the NO bioavailability in the animals (Figure 12.). These results suggest, that in chronic kidney disease, uremia decreases the ACh-induced relaxation of the vessels as well as the basal NO bioavailability and only the first can be recovered by syn-mmu-miR-142-3p treatment.

It is described in the literature that microRNA-142-3p has a role in hematopoietic differentiation and maturation (173-175). These effects of microRNA-142-3p should be considered when using it as a pharmacological agent. For this reason we prepared differential hemograms from the mice at the end of the experiments after eleven days of high phosphate diet. We found no difference in red blood cell or thrombocyte numbers, however syn-mmu-miR-142-3p treatment had a clear effect on white blood cell numbers. Granulocyte numbers decreased whereas lymphocyte and monocyte numbers significantly increased 48 hours after the syn-mmu-miR-142-3p treatment (Figure 13.).

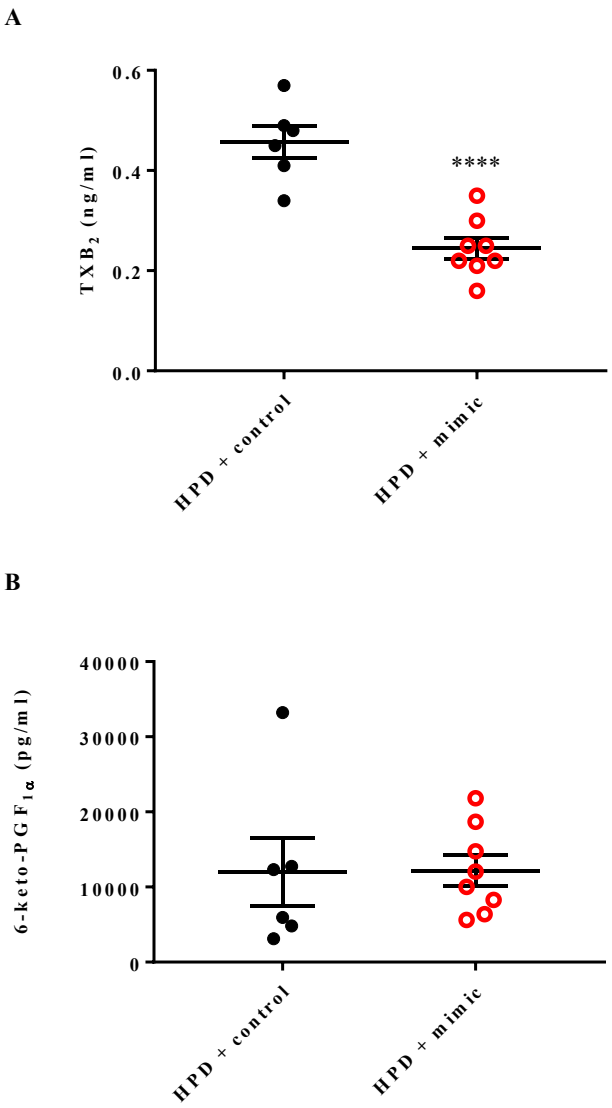

Figure 8.

Syn-mmu-miR-142-3p reduces thromboxane synthesis

DBA/2 mice were either fed high-phosphate diet (HPD) and were treated with syn-mmu-miR-142-3p mimic or negative control siRNA 48 hours before the end of the experiment. Animals were divided into two treatment groups: HPD with control injection (closed circles), and HPD with mimic injection (red open circles). The thromboxane B2 synthesis (TXB2) was significantly reduced in explanted aortic rings after treatment with syn-mmu-miR-142-3p mimic injection (A). 6-keto-$PGF_{1\alpha}$ synthesis was not affected by the syn-mmu-miR-142-3p treatment. Data represent mean ± SEM. ****indicates $p < 0.0001$. Data shown in this figure was previously published (1).

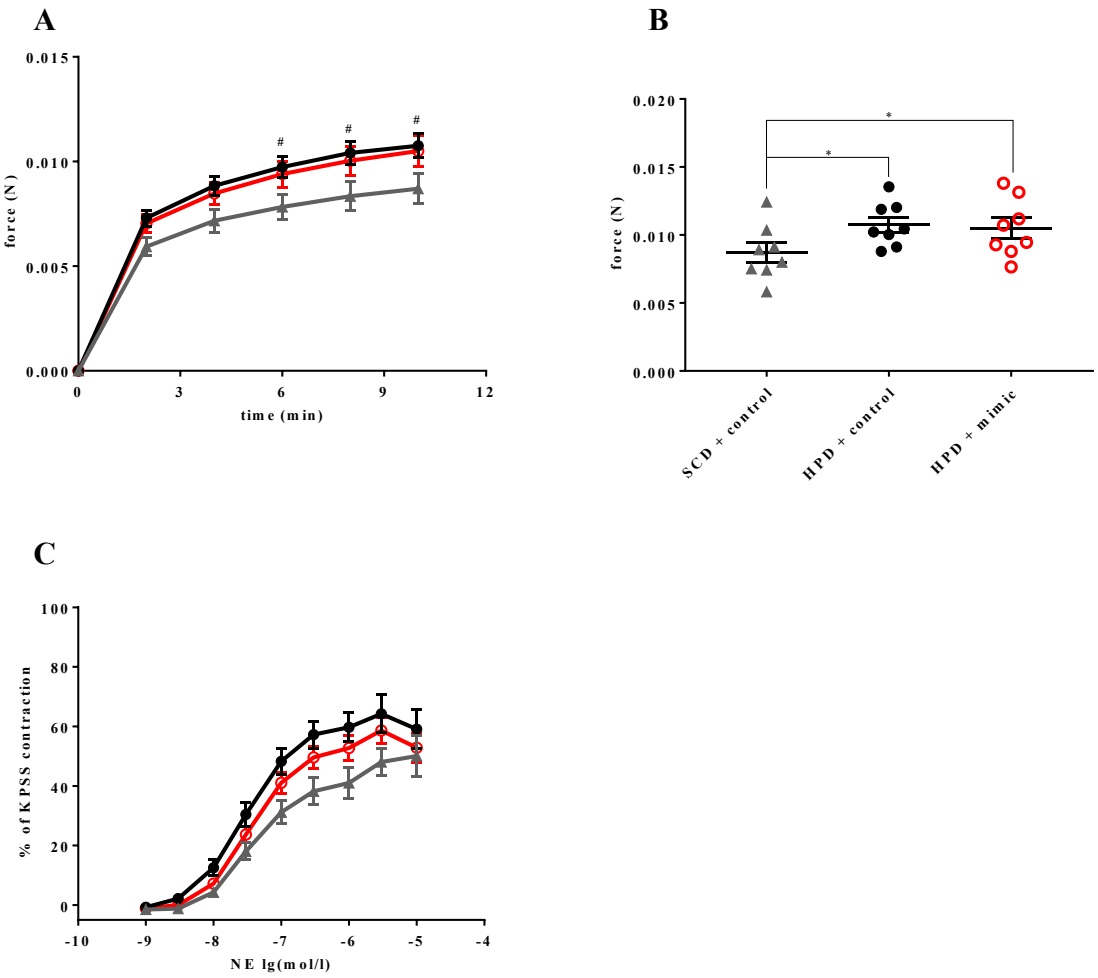

Figure 9.

Effects of high phosphate diet on aortic contraction in the presence of diclofenac

DBA/2 mice were either fed standard chow (SCD) or high-phosphate diet (HPD) and were treated with syn-mmu-miR-142-3p mimic or negative control siRNA 48 hours before the end of the experiment. Animals were divided into 3 treatment groups: SCD with control injection (grey closed triangles), HPD with control injection (closed circles), and HPD with mimic injection (red open circles). KPSS contraction over time (A), maximum KPSS contraction force (B) and norepinephrine-induced contraction (C) were evaluated in all treatment groups in the presence of 10 μM diclofenac. Data represent mean ± SEM. * indicates *$p < 0.05$ between mice on HPD that were treated either by injection of syn-mmu-miR-142-3p mimic or negative control siRNA. # indicates $p < 0.05$ between HPD + control and SCD + control groups. Data shown in this figure was previously published (1).

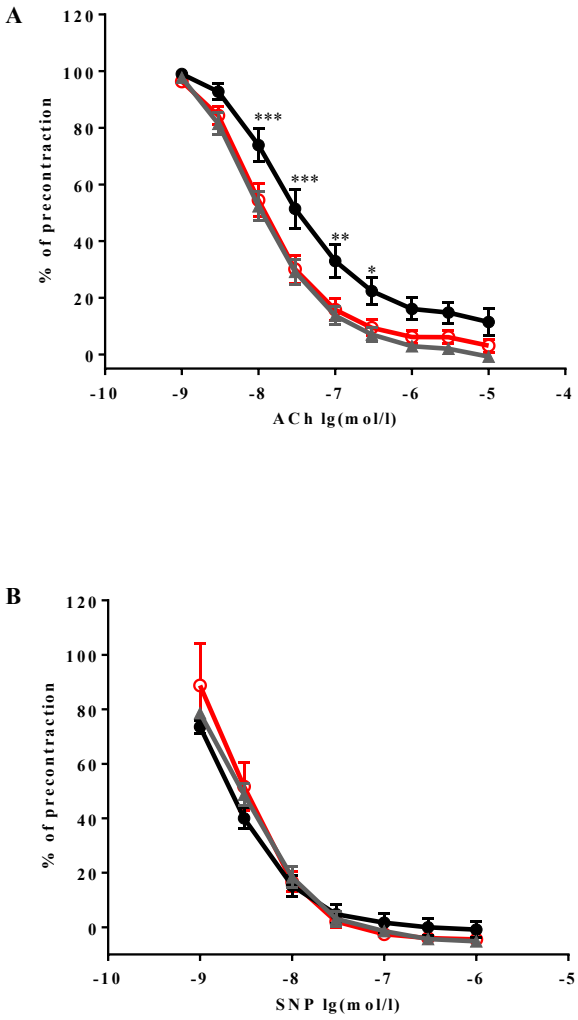

Figure 10.

Diclofenac treatment does not abolish the effect of syn-mmu-mir-142-3p on relaxation

DBA/2 mice were either fed standard chow (SCD) or high-phosphate diet (HPD) and were treated with syn-mmu-miR-142-3p mimic or negative control siRNA 48 hours before the end of the experiment. Animals were divided into 3 treatment groups: SCD with control injection (grey closed triangles), HPD with control minjection (closed circles), and HPD with mimic injection (red open circles). Acetylcholine (ACh)-induced relaxation of NE-precontracted aortic rings (A) and sodium nitroprusside (SNP)-mediated relaxation of NE-precontracted aortic rings (B) were evaluated in the presence of 10 µM diclofenac. Data represent mean ± SEM. * indicates *$p < 0.05$, **$p < 0.01$ and ***$p < 0.001$ between mice on HPD that were treated either by injection of syn-mmu-miR-142-3p mimic or negative control siRNA. Data shown in this figure was previously published (1).

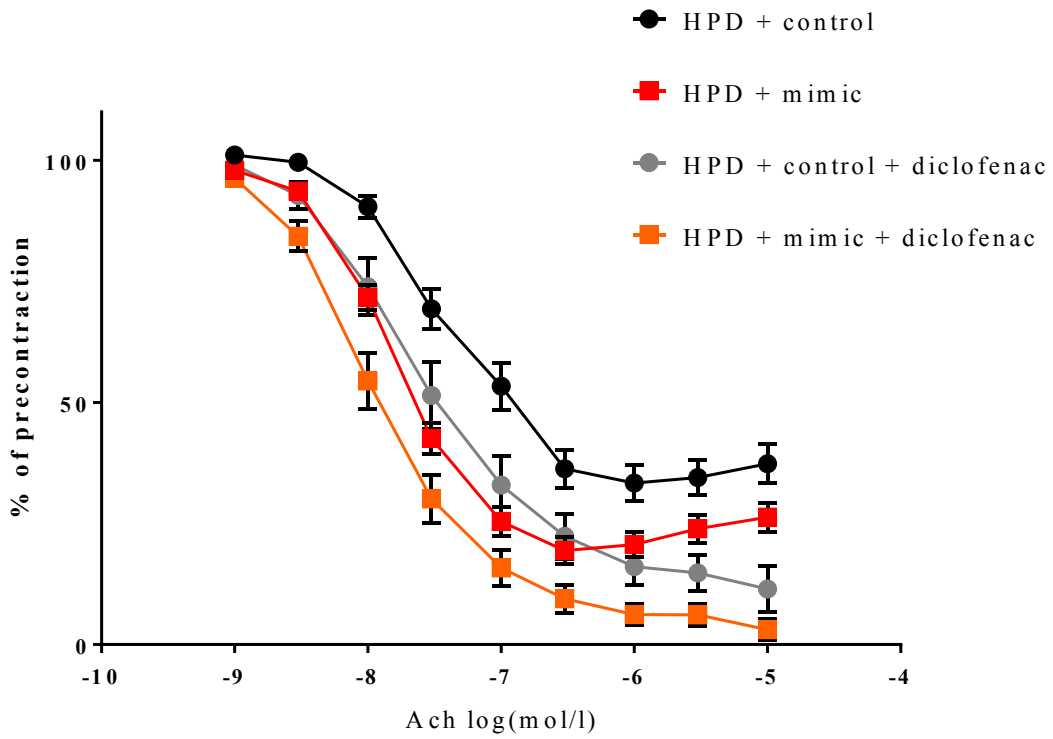

	HPD + control	HPD + mimic	HPD + control + diclofenac	HPD + mimic + diclofenac
LogIC50	-7.473	-7.916	-7.645	-8.004
IC50	3.369e-008	1.212e-008	2.264e-008	9.904e-009

Figure 11.

The extent of thromboxane mediated effect of miR-142-3p on relaxation

DBA/2 mice were fed high-phosphate diet (HPD) for 11 days and were treated with syn-mmu-miR-142-3p mimic or negative control siRNA 48 hours before the end of the experiment. The effect of syn-mmu-miR-142-3p on acetylcholine (ACh)-induced relaxation of NE-precontracted aortic rings was measured in the presence or in the absence of diclofenac (10 μM). Samples were divided into 4 treatment groups: HPD with control injection (black closed circles), HPD with mimic injection (red closed squares), HPD with control injection, measured in the presence of diclofenac (grey closed circles), and HPD with mimic injection, measured in the presence of diclofenac (orange closed squares). IC50 values were calculated via nonlinear regression curve fitting and were significantly different in all four groups ($p < 0.001$). Data shown in this figure was previously published (1).

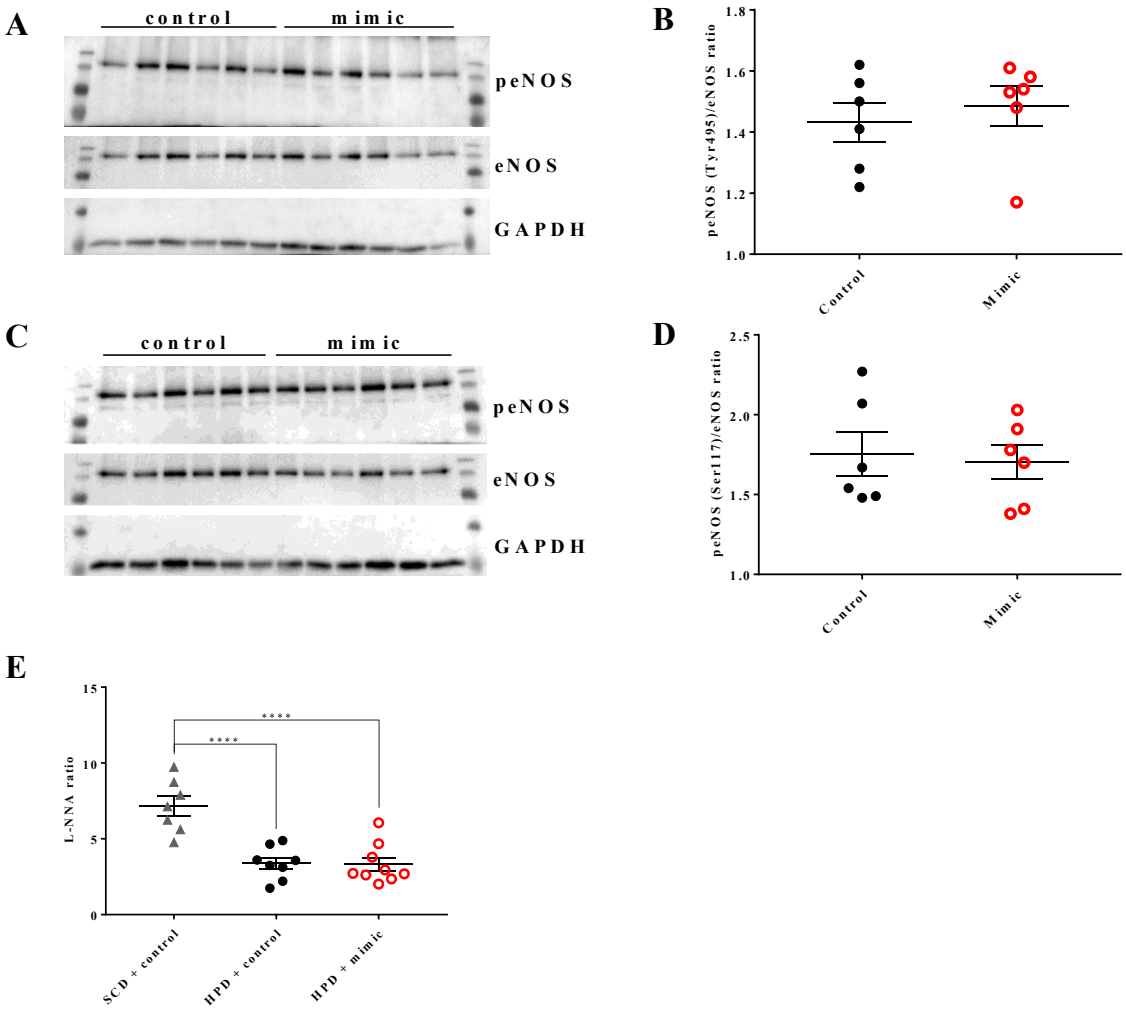

Figure 12.

MiR-142-3p treatment does not affect NO bioavailability or eNOS phosphorilation

DBA/2 mice were fed high-phosphate diet (HPD) and were treated with syn-mmu-miR-142-3p mimic or negative control siRNA 48 hours before the end of the experiment. Aortas from the mice were isolated, cut into 2 mm rings, then treated with 10 µM acetylcholine for 10 minutes. Endothelial nitric oxide synthase (eNOS) phosphorilation was evaulated by Western blot for Tyr495 inhibitory (A) and Ser1177 activating (B) phosphorilation sites. Densitometric analyses were performed for quantification (C and D). The L-nitroarginine (L-NNA)-induced endothelium-dependent constriction response in NE-preconstricted aortic rings was evaluated via wire myography (E). Data shown in this figure was previously published (1).

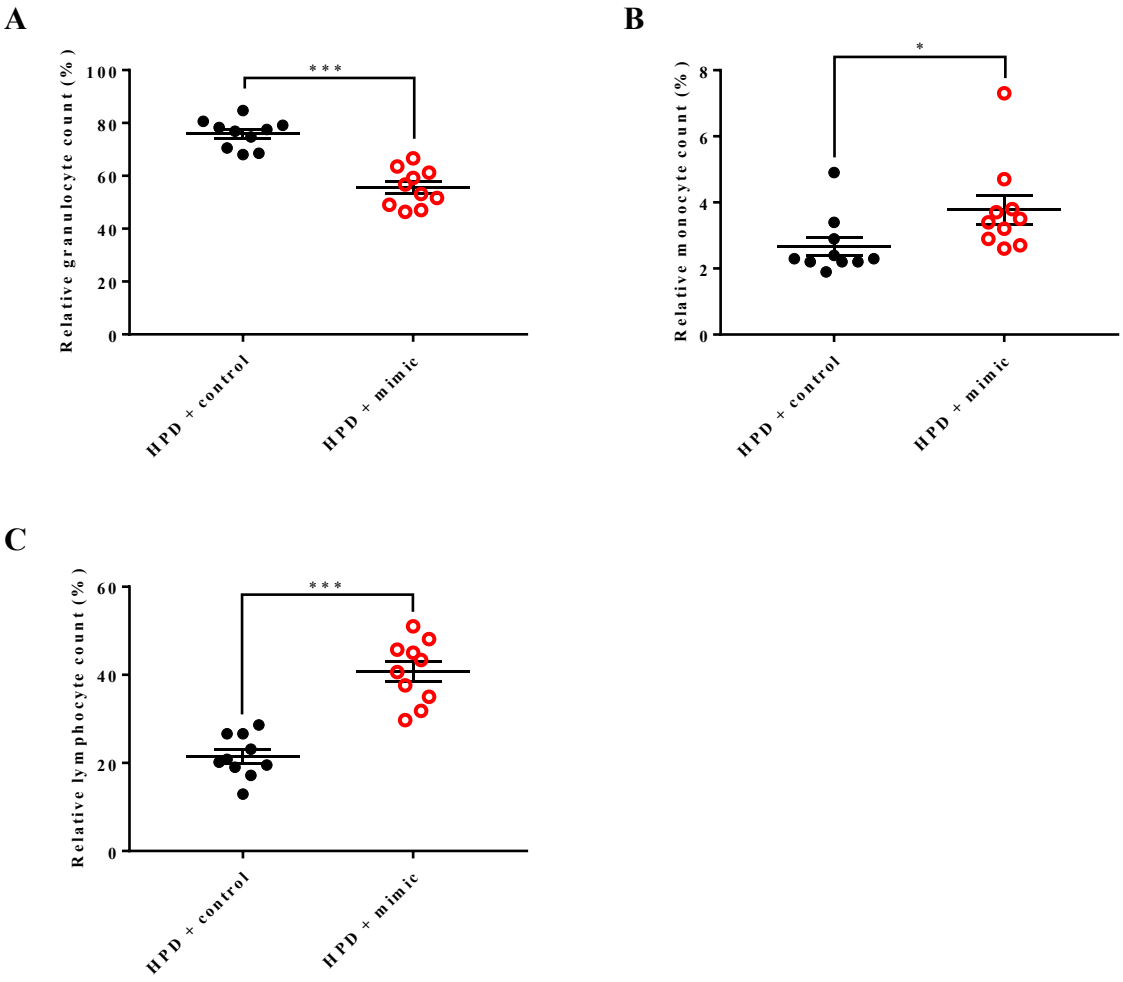

Figure 13.

MiR-142-3p treatment affects white blood cell numbers

DBA/2 mice were high-phosphate diet (HPD) and were treated with syn-mmu-miR-142-3p mimic or negative control siRNA 48 hours before a differential hemogram was made. Syn-mmu-miR-142-3p decreased the granulocyte numbers (A) and increased the monocyte and lymphocyte counts (B and C). * indicates *$p < 0.05$ and ***$p < 0.001$.

Discussion

Chronic kidney disease is a severe and common condition. The prevalence of chronic kidney disease is 13,4% in the world and CKD stage 3-5 affects 10,6% of the population (25). The primary cause of morbidity and mortality in chronic kidney disease is cardiovascular disease and chronic kidney disease is tightly associated with an increased risk of cardiovascular morbidity and mortality (1, 66). The risk of cardiovascular disease and cardiovascular mortatily is increased in end-stage renal disease (ESRD) patients 10-100-fold compared to patients with intact kidney function. Extensive research on the role of microRNAs in chronic kidney disease associated vascular disease is lacking. However microRNA research is quickly expanding, especially on different types of cancer.

More and more microRNAs provide promising targets in the treatment of several diseases and microRNA delivery possibilities are also expanding. There are already clinical trials in phase I and phase II stages, investigating the potential clinical use of microRNA therapies. However, miRNA therapies in cardiovascular diseases are only investigated in cardiac diseases and to our knowledge no microRNA therapy was investigated in the treatment of endothelial dysfunction so far. In this study, we used the state of the art in vivo JetPEI method to deliver the synthetich microRNA-142-3p mimic in vivo and provided a promising target for further research in the treatment of endothelial dysfunction in chronic kidney disease.

Vascular tone is regulated by the endothelium via different regulators which maintain the balance between vasodilatation an vasoconstriction (176). In this thesis we provide evidence that microRNAs are involved in uremic endothelial dysfunction. Our result show that blood microRNA-142-3p levels are negatively associated with carotid-femoral pulsewave velocity in end-stage renal disease patients, which is a marker for arterial stiffnes and a prognostic factor for cardiovascular morbidity and mortality. Decreased microRNA-142-3p levels might play a pathogenic role in chronic kidney disease both in humans and in mice, since restoring microRNA-142-3p bioavailability improved ACh-mediated vascular relaxation in uremic DBA/2 mice (1).

So far the effects of miR-142-3p were mainly investigated in different types of cancers (177-183). To our knowledge, in this study we provide the first direct functional evidence of an in vivo effect of microRNA treatment in uremic vascular disease. We further extend the previous findings of Zhang et al., who showed that the expression of eNOS in human peripheral blood-derived endothelial progenitor cells are promoted by microRNA-142 in vitro (184). Moreover, our results also support the findings of Sharma et al., who showed that microRNA-142-3p and microRNA-142-5p play a critical role in the adaptation to hemodynamic stress in adaptive cardiac hypertrophy (116).

In this thesis, we provide proof that microRNA-142-3p is not just a mere biomarker of chronic kidney disease and endothelial dysfunction, but rather plays a direct, functional role in vascular relaxation. It is also a mediator of impaired ACh-mediated vascular relaxation in end-stage renal disease and uremia. MicroRNA-142-3p could present a potential pharmacological target in the prevention of the arterial stiffness in uremia.

In uremic conditions there are profound vascular changes which have large-scale effects on endothelial cells as well as on vascular smooth muscle cells. These vascular changes are associated with an increased risk of cardiovascular morbidity and mortality (66-69). Several microRNAs are already described as biomarkers or regulators in vascular calfication and in this study we provide a list of microRNAs which could act as biomarkers or have a functional role in chronic kidney disease and vascular disfunction as well (185-193). Our results corroborate the findings of Goettsch et al. who found miR-125b to be significantly downregulated in human coronary smooth muscle cells after 21 days of calcifying conditions. In apolipoprotein E knockout mice, they also found that miR-125b was downregulated in the calcified aortas (192).

Evidence about the functional role of microRNAs in vessel impairment during uremia is only beginning to emerge. Our results support the findings of Shang et al. who showed that uremic serum could induces microRNA-92 expression in vitro in cultured endothelial cells. They also found that microRNA-92 is associated with uremic toxin levels in chronic kidney disease patients (1, 194).

The exact mode of action of microRNA-142-3p in ACh-mediated vascular relaxation is not yet fully understood. Partly it is attributable to the attenuation of thromboxane A2 signaling, which is a potent vasoconstrictor and it does not affect the vasodilatator prostacyclin pathway. Restoring microRNA-142-3p levels in vivo did not affect the basal NO bioavailability, as shown by the L-NNA-induced endothelium-dependent constrictor response in NE-preconstricted aortic rings. Also neither decreased inhibitory Tyr495, nor increased activating Ser1177 eNOS phosphorylation played a role in the increased ACh-mediated relaxation in our animal model. However, our results and experiments do not exclude an augmented NO bioavailability after endothelial activation in vivo. An increased activation or induction of the eNOS pathway due to altered intracellular localisation of eNOS or a higher efficacy of ACh-mediated signalling could also contribute to the protective effects of the syn-mmu-miR-142-3p treatment on vascular relaxation in uremic conditions.

MicroRNA-142-3p also plays a role in the maturation of T cells and in hematopoietic lineage formation (173-175). We also found that granulocyte numbers decreased whereas lymphocyte and monocyte numbers significantly increased 48 hours after the syn-mmu-miR-142-3p treatment. These effects of microRNA-142-3p should be considered when using it as a pharmacological agent and might limit its therapeutic applications. These potential additional effects deserve further evaluation, especially when considering long-term therapeutic treatments with synthetic miR-142-3p mimics.

The small sample size of the healthy, control cohort and the limited number of end-stage renal disease patients who underwent kidney transplantation and were controlled after one year constitutes a limitation of this study. Further investigation is needed on larger cohorts in order to safely determine the exact extent of microRNA-142-3p as a biomarker and pharmacological tool in end-stage renal disease.

In our experiments, the pharmacological intervention with intravenous injecton of the synthethic microRNA-142-3p mimic did not affect the degree of vascular calcification in our animal model. This finding reflects also the human data, where we did not find any association of microRNA-142-3p blood levels with vascular calcification which was assessed by computed tomography. However we found that blood microRNA-142-3p levels were negatively associated with carotid-femoral pulse wave velocity and in our animal model synthethic microRNA-142-3p mimic injections ameliorated the impaired ACh-mediated endothelium dependent vascular relaxation. Our different findings on

morphological and functional levels in uremic vessels highlight the fact that endothelial dysfunction with impaired ACh-mediated vascular relaxation significantly contributes to arterial stiffness and may precede morphological changes in the tunica media with VSMC phenotypic transdifferentiation. In fact, the microRNA profile was reversible in the subgroup of patients after kidney transplantation and this change was independent of age, dialysis vintage or dialysis modality.

Taken together, pharmacological exploitation of naturally occurring microRNAs and especially microRNA-142-3p could be a potential avenue to counteract vascular dysfunction in uremia and might thus ultimately prevent deleterious cardiovascular endpoints in patients with end-stage renal disease (1).

Outlook

The first microRNA was discovered in 1993 and microRNA research quicky expanded after 2000. Several researchers made significant contributions to this field which helped to understand the general mode of action of these molecules. Despite the remarkable advances in microRNA research, there is still only limited amount of data available about microRNA involvement in human diseases.

In this study we identified details of the microRNA-142-3p signaling pathway in chronic kidney disease, but our understanding of the exact pathomechanism is still restricted. Further research should focus on finding the RNA molecule which acts as the first step in the pathway. Also the mode of action of microRNA-142-3p is not solely attributable to its effect on thromboxane levels, additional investigation should focus on finding other molecules which contribute to the patomechanism.

The low number of patients constitutes a limitation to this study, it should be considered to enroll patients from different centers and evaluate their microRNA expression patterns as well. Also it should be assessed whether expanding the investigated microRNA panel would yield further potential biomarkers and pharmaceutical targets which could help in the early diagnosis and treatment in chronic kidney disease and vascular calcification.

The research performed on microRNAs in human diseases helps expanding our knowledge on their mode of action and might reveal patomechanisms which are not yet described. The highly interdisciplinary approach provides an excellent oppurtinity for researchers and clinicians to solve this problem together.

Bibliography

1. Ketszeri M, Kirsch A, Frauscher B, Moschovaki-Filippidou F, Mooslechner AA, Kirsch AH, et al. MicroRNA-142-3p improves vascular relaxation in uremia. Atherosclerosis. 2018;280:28-36.

2. Levin A, Stevens PE. Summary of KDIGO 2012 CKD Guideline: behind the scenes, need for guidance, and a framework for moving forward. Kidney international. 2014;85(1):49-61.

3. de Boer IH. A New Chapter for Diabetic Kidney Disease. The New England journal of medicine. 2017;377(9):885-7.

4. Mora-Fernandez C, Dominguez-Pimentel V, de Fuentes MM, Gorriz JL, Martinez-Castelao A, Navarro-Gonzalez JF. Diabetic kidney disease: from physiology to therapeutics. The Journal of physiology. 2014;592(18):3997-4012.

5. Cao Z, Cooper ME. Pathogenesis of diabetic nephropathy. J Diabetes Investig. 2011;2(4):243-7.

6. Kimmelstiel P, Wilson C. Intercapillary Lesions in the Glomeruli of the Kidney. The American journal of pathology. 1936;12(1):83-98 7.

7. Kazancioglu R. Risk factors for chronic kidney disease: an update. Kidney international supplements. 2013;3(4):368-71.

8. Lea JP, Nicholas SB. Diabetes mellitus and hypertension: key risk factors for kidney disease. Journal of the National Medical Association. 2002;94(8 Suppl):7S-15S.

9. Bruno G, Merletti F, Bargero G, Novelli G, Melis D, Soddu A, et al. Estimated glomerular filtration rate, albuminuria and mortality in type 2 diabetes: the Casale Monferrato study. Diabetologia. 2007;50(5):941-8.

10. McClellan WM, Flanders WD. Risk factors for progressive chronic kidney disease. Journal of the American Society of Nephrology : JASN. 2003;14(7 Suppl 2):S65-70.

11. Fogo AB. Hypertensive risk factors in kidney disease in African Americans. Kidney international Supplement. 2003(83):S17-21.

12. Rowe DJ, Bagga H, Betts PB. Normal variations in rate of albumin excretion and albumin to creatinine ratios in overnight and daytime urine collections in non-diabetic children. British medical journal. 1985;291(6497):693-4.

13. Cornec-Le Gall E, Le Meur Y. [Autosomal dominant polycystic kidney disease: is the treatment for tomorrow?]. Nephrologie & therapeutique. 2014;10(6):433-40.

14. Levy M, Feingold J. Estimating prevalence in single-gene kidney diseases progressing to renal failure. Kidney international. 2000;58(3):925-43.

15. Torres VE, Harris PC, Pirson Y. Autosomal dominant polycystic kidney disease. Lancet. 2007;369(9569):1287-301.

16. Murray TG, Goldberg M. Analgesic-associated nephropathy in the U.S.A.: epidemiologic, clinical and pathogenetic features. Kidney international. 1978;13(1):64-71.

17. Feinstein AR, Heinemann LA, Curhan GC, Delzell E, Deschepper PJ, Fox JM, et al. Relationship between nonphenacetin combined analgesics and nephropathy: a review. Ad Hoc Committee of the International Study Group on Analgesics and Nephropathy. Kidney international. 2000;58(6):2259-64.

18. Maisonneuve P, Agodoa L, Gellert R, Stewart JH, Buccianti G, Lowenfels AB, et al. Distribution of primary renal diseases leading to end-stage renal failure in the United States, Europe, and Australia/New Zealand: results from an international comparative study. American journal of kidney diseases : the official journal of the National Kidney Foundation. 2000;35(1):157-65.

19. Nanra RS, Stuart-Taylor J, de Leon AH, White KH. Analgesic nephropathy: etiology, clinical syndrome, and clinicopathologic correlations in Australia. Kidney international. 1978;13(1):79-92.

20. Levey AS, Coresh J, Balk E, Kausz AT, Levin A, Steffes MW, et al. National Kidney Foundation practice guidelines for chronic kidney disease: evaluation, classification, and stratification. Annals of internal medicine. 2003;139(2):137-47.

21. Levey AS, Eckardt KU, Tsukamoto Y, Levin A, Coresh J, Rossert J, et al. Definition and classification of chronic kidney disease: a position statement from Kidney Disease: Improving Global Outcomes (KDIGO). Kidney international. 2005;67(6):2089-100.

22. National Kidney F. K/DOQI clinical practice guidelines for chronic kidney disease: evaluation, classification, and stratification. American journal of kidney diseases : the official journal of the National Kidney Foundation. 2002;39(2 Suppl 1):S1-266.

23. Levey AS, Stevens LA, Coresh J. Conceptual model of CKD: applications and implications. American journal of kidney diseases : the official journal of the National Kidney Foundation. 2009;53(3 Suppl 3):S4-16.

24. Stevens PE, Levin A, Kidney Disease: Improving Global Outcomes Chronic Kidney Disease Guideline Development Work Group M. Evaluation and management of chronic kidney disease: synopsis of the kidney disease: improving global outcomes 2012 clinical practice guideline. Annals of internal medicine. 2013;158(11):825-30.

25. Hill NR, Fatoba ST, Oke JL, Hirst JA, O'Callaghan CA, Lasserson DS, et al. Global Prevalence of Chronic Kidney Disease - A Systematic Review and Meta-Analysis. PloS one. 2016;11(7):e0158765.

26. Chang A, Kramer H. CKD progression: a risky business. Nephrology, dialysis, transplantation : official publication of the European Dialysis and Transplant Association - European Renal Association. 2012;27(7):2607-9.

27. Ejerblad E, Fored CM, Lindblad P, Fryzek J, McLaughlin JK, Nyren O. Obesity and risk for chronic renal failure. Journal of the American Society of Nephrology : JASN. 2006;17(6):1695-702.

28. Ravera M, Re M, Deferrari L, Vettoretti S, Deferrari G. Importance of blood pressure control in chronic kidney disease. Journal of the American Society of Nephrology : JASN. 2006;17(4 Suppl 2):S98-103.

29. Tozawa M, Iseki K, Iseki C, Kinjo K, Ikemiya Y, Takishita S. Blood pressure predicts risk of developing end-stage renal disease in men and women. Hypertension. 2003;41(6):1341-5.

30. Luyckx VA, Brenner BM. The clinical importance of nephron mass. Journal of the American Society of Nephrology : JASN. 2010;21(6):898-910.

31. Vikse BE, Irgens LM, Leivestad T, Hallan S, Iversen BM. Low birth weight increases risk for end-stage renal disease. Journal of the American Society of Nephrology : JASN. 2008;19(1):151-7.

32. Harris PC, Torres VE. Polycystic Kidney Disease, Autosomal Dominant. In: Adam MP, Ardinger HH, Pagon RA, Wallace SE, Bean LJH, Stephens K, et al., editors. GeneReviews((R)). Seattle (WA)1993.

33. Atkinson MA, Warady BA. Anemia in chronic kidney disease. Pediatric nephrology. 2018;33(2):227-38.

34. Mikhail A, Brown C, Williams JA, Mathrani V, Shrivastava R, Evans J, et al. Renal association clinical practice guideline on Anaemia of Chronic Kidney Disease. BMC nephrology. 2017;18(1):345.

35. Del Vecchio L, Locatelli F. Roxadustat in the treatment of anaemia in chronic kidney disease. Expert opinion on investigational drugs. 2018;27(1):125-33.

36. Soi V, Yee J. Sodium Homeostasis in Chronic Kidney Disease. Advances in chronic kidney disease. 2017;24(5):325-31.

37. Ellison DH. Treatment of Disorders of Sodium Balance in Chronic Kidney Disease. Advances in chronic kidney disease. 2017;24(5):332-41.

38. Salerno FR, Parraga G, McIntyre CW. Why Is Your Patient Still Short of Breath? Understanding the Complex Pathophysiology of Dyspnea in Chronic Kidney Disease. Seminars in dialysis. 2017;30(1):50-7.

39. Moe S, Drueke T, Cunningham J, Goodman W, Martin K, Olgaard K, et al. Definition, evaluation, and classification of renal osteodystrophy: a position statement from Kidney Disease: Improving Global Outcomes (KDIGO). Kidney international. 2006;69(11):1945-53.

40. Frauscher B, Artinger K, Kirsch AH, Aringer I, Moschovaki-Filippidou F, Ketszeri M, et al. A New Murine Model of Chronic Kidney Disease-Mineral and Bone Disorder. International journal of endocrinology. 2017;2017:1659071.

41. Frauscher B, Kirsch AH, Schabhuttl C, Schweighofer K, Ketszeri M, Pollheimer M, et al. Autophagy Protects From Uremic Vascular Media Calcification. Frontiers in immunology. 2018;9:1866.

42. Ketteler M, Gross ML, Ritz E. Calcification and cardiovascular problems in renal failure. Kidney international Supplement. 2005(94):S120-7.

43. London GM, Marchais SJ, Guerin AP, Metivier F. Arteriosclerosis, vascular calcifications and cardiovascular disease in uremia. Current opinion in nephrology and hypertension. 2005;14(6):525-31.

44. Vervloet M, Cozzolino M. Vascular calcification in chronic kidney disease: different bricks in the wall? Kidney international. 2017;91(4):808-17.

45. Amann K. Media calcification and intima calcification are distinct entities in chronic kidney disease. Clinical journal of the American Society of Nephrology : CJASN. 2008;3(6):1599-605.

46. Drueke TB. Arterial intima and media calcification: distinct entities with different pathogenesis or all the same? Clinical journal of the American Society of Nephrology : CJASN. 2008;3(6):1583-4.

47. Koleganova N, Piecha G, Ritz E, Schirmacher P, Muller A, Meyer HP, et al. Arterial calcification in patients with chronic kidney disease. Nephrology, dialysis, transplantation : official publication of the European Dialysis and Transplant Association - European Renal Association. 2009;24(8):2488-96.

48. Usman A, Ribatti D, Sadat U, Gillard JH. From Lipid Retention to Immune-Mediate Inflammation and Associated Angiogenesis in the Pathogenesis of Atherosclerosis. J Atheroscler Thromb. 2015;22(8):739-49.

49. Otsuka F, Sakakura K, Yahagi K, Joner M, Virmani R. Has our understanding of calcification in human coronary atherosclerosis progressed? Arteriosclerosis, thrombosis, and vascular biology. 2014;34(4):724-36.

50. Cozzolino M, Brancaccio D, Gallieni M, Slatopolsky E. Pathogenesis of vascular calcification in chronic kidney disease. Kidney international. 2005;68(2):429-36.

51. London G, Covic A, Goldsmith D, Wiecek A, Suleymanlar G, Ortiz A, et al. Arterial aging and arterial disease: interplay between central hemodynamics, cardiac work, and organ flow-implications for CKD and cardiovascular disease. Kidney international supplements. 2011;1(1):10-2.

52. Foley RN, Parfrey PS, Sarnak MJ. Clinical epidemiology of cardiovascular disease in chronic renal disease. American journal of kidney diseases : the official journal of the National Kidney Foundation. 1998;32(5 Suppl 3):S112-9.

53. Foley RN, Parfrey PS, Sarnak MJ. Epidemiology of cardiovascular disease in chronic renal disease. Journal of the American Society of Nephrology : JASN. 1998;9(12 Suppl):S16-23.

54. Shroff RC, McNair R, Figg N, Skepper JN, Schurgers L, Gupta A, et al. Dialysis accelerates medial vascular calcification in part by triggering smooth muscle cell apoptosis. Circulation. 2008;118(17):1748-57.

55. Pai A, Leaf EM, El-Abbadi M, Giachelli CM. Elastin degradation and vascular smooth muscle cell phenotype change precede cell loss and arterial medial calcification in a uremic mouse model of chronic kidney disease. The American journal of pathology. 2011;178(2):764-73.

56. Ciceri P, Volpi E, Brenna I, Arnaboldi L, Neri L, Brancaccio D, et al. Combined effects of ascorbic acid and phosphate on rat VSMC osteoblastic differentiation. Nephrology, dialysis, transplantation : official publication of the European Dialysis and Transplant Association - European Renal Association. 2012;27(1):122-7.

57. Shanahan CM, Crouthamel MH, Kapustin A, Giachelli CM. Arterial calcification in chronic kidney disease: key roles for calcium and phosphate. Circulation research. 2011;109(6):697-711.

58. Adeney KL, Siscovick DS, Ix JH, Seliger SL, Shlipak MG, Jenny NS, et al. Association of serum phosphate with vascular and valvular calcification in moderate CKD. Journal of the American Society of Nephrology : JASN. 2009;20(2):381-7.

59. Cancela AL, Santos RD, Titan SM, Goldenstein PT, Rochitte CE, Lemos PA, et al. Phosphorus is associated with coronary artery disease in patients with preserved renal function. PloS one. 2012;7(5):e36883.

60. Dhingra R, Sullivan LM, Fox CS, Wang TJ, D'Agostino RB, Sr., Gaziano JM, et al. Relations of serum phosphorus and calcium levels to the incidence of cardiovascular disease in the community. Arch Intern Med. 2007;167(9):879-85.

61. Kestenbaum B, Sampson JN, Rudser KD, Patterson DJ, Seliger SL, Young B, et al. Serum phosphate levels and mortality risk among people with chronic kidney disease. Journal of the American Society of Nephrology : JASN. 2005;16(2):520-8.

62. Barreto DV, Barreto FC, Liabeuf S, Temmar M, Boitte F, Choukroun G, et al. Vitamin D affects survival independently of vascular calcification in chronic kidney disease. Clinical journal of the American Society of Nephrology : CJASN. 2009;4(6):1128-35.

63. Lim K, Lu TS, Molostvov G, Lee C, Lam FT, Zehnder D, et al. Vascular Klotho deficiency potentiates the development of human artery calcification and mediates resistance to fibroblast growth factor 23. Circulation. 2012;125(18):2243-55.

64. Leonard O, Spaak J, Goldsmith D. Regression of vascular calcification in chronic kidney disease - feasible or fantasy? a review of the clinical evidence. Br J Clin Pharmacol. 2013;76(4):560-72.

65. Yazbek DC, de Carvalho AB, Barros CS, Medina Pestana JO, Canziani ME. Effect of Statins on the Progression of Coronary Calcification in Kidney Transplant Recipients. PloS one. 2016;11(4):e0151797.

66. Go AS, Chertow GM, Fan D, McCulloch CE, Hsu CY. Chronic kidney disease and the risks of death, cardiovascular events, and hospitalization. The New England journal of medicine. 2004;351(13):1296-305.

67. Sarnak MJ, Levey AS, Schoolwerth AC, Coresh J, Culleton B, Hamm LL, et al. Kidney disease as a risk factor for development of cardiovascular disease: a statement from the American Heart Association Councils on Kidney in Cardiovascular Disease, High Blood Pressure Research, Clinical Cardiology, and Epidemiology and Prevention. Circulation. 2003;108(17):2154-69.

68. Wilson PW, Kauppila LI, O'Donnell CJ, Kiel DP, Hannan M, Polak JM, et al. Abdominal aortic calcific deposits are an important predictor of vascular morbidity and mortality. Circulation. 2001;103(11):1529-34.

69. Witteman JC, Kok FJ, van Saase JL, Valkenburg HA. Aortic calcification as a predictor of cardiovascular mortality. Lancet. 1986;2(8516):1120-2.

70. Blacher J, Guerin AP, Pannier B, Marchais SJ, London GM. Arterial calcifications, arterial stiffness, and cardiovascular risk in end-stage renal disease. Hypertension. 2001;38(4):938-42.

71. Kopel T, Kaufman JS, Hamburg N, Sampalis JS, Vita JA, Dember LM. Endothelium-Dependent and -Independent Vascular Function in Advanced Chronic Kidney Disease. Clinical journal of the American Society of Nephrology : CJASN. 2017;12(10):1588-94.

72. Fellstrom BC, Jardine AG, Schmieder RE, Holdaas H, Bannister K, Beutler J, et al. Rosuvastatin and cardiovascular events in patients undergoing hemodialysis. The New England journal of medicine. 2009;360(14):1395-407.

73. Karumanchi SA, Thadhani R. Kidney complications: why don't statins always work? Nature medicine. 2010;16(1):38-40.

74. Wanner C, Krane V, Marz W, Olschewski M, Mann JF, Ruf G, et al. Atorvastatin in patients with type 2 diabetes mellitus undergoing hemodialysis. The New England journal of medicine. 2005;353(3):238-48.

75. Jourde-Chiche N, Dou L, Cerini C, Dignat-George F, Brunet P. Vascular incompetence in dialysis patients--protein-bound uremic toxins and endothelial dysfunction. Seminars in dialysis. 2011;24(3):327-37.

76. Paloian NJ, Giachelli CM. A current understanding of vascular calcification in CKD. American journal of physiology Renal physiology. 2014;307(8):F891-900.

77. Ambros V. The functions of animal microRNAs. Nature. 2004;431(7006):350-5.

78. Bartel DP. MicroRNAs: genomics, biogenesis, mechanism, and function. Cell. 2004;116(2):281-97.

79. Bartel DP. Metazoan MicroRNAs. Cell. 2018;173(1):20-51.

80. Lagos-Quintana M, Rauhut R, Lendeckel W, Tuschl T. Identification of novel genes coding for small expressed RNAs. Science. 2001;294(5543):853-8.

81. Lau NC, Lim LP, Weinstein EG, Bartel DP. An abundant class of tiny RNAs with probable regulatory roles in Caenorhabditis elegans. Science. 2001;294(5543):858-62.

82. Lee RC, Ambros V. An extensive class of small RNAs in Caenorhabditis elegans. Science. 2001;294(5543):862-4.

83. Pasquinelli AE, Reinhart BJ, Slack F, Martindale MQ, Kuroda MI, Maller B, et al. Conservation of the sequence and temporal expression of let-7 heterochronic regulatory RNA. Nature. 2000;408(6808):86-9.

84. Reinhart BJ, Slack FJ, Basson M, Pasquinelli AE, Bettinger JC, Rougvie AE, et al. The 21-nucleotide let-7 RNA regulates developmental timing in Caenorhabditis elegans. Nature. 2000;403(6772):901-6.

85. Fasanaro P, Greco S, Ivan M, Capogrossi MC, Martelli F. microRNA: emerging therapeutic targets in acute ischemic diseases. Pharmacology & therapeutics. 2010;125(1):92-104.

86. Hydbring P, Badalian-Very G. Clinical applications of microRNAs. F1000Research. 2013;2:136.

87. Feng J, Sun G, Yan J, Noltner K, Li W, Buzin CH, et al. Evidence for X-chromosomal schizophrenia associated with microRNA alterations. PloS one. 2009;4(7):e6121.

88. Trang P, Weidhaas JB, Slack FJ. MicroRNAs as potential cancer therapeutics. Oncogene. 2008;27 Suppl 2:S52-7.

89. Krol J, Sobczak K, Wilczynska U, Drath M, Jasinska A, Kaczynska D, et al. Structural features of microRNA (miRNA) precursors and their relevance to miRNA biogenesis and small interfering RNA/short hairpin RNA design. The Journal of biological chemistry. 2004;279(40):42230-9.

90. Rana TM. Illuminating the silence: understanding the structure and function of small RNAs. Nature reviews Molecular cell biology. 2007;8(1):23-36.

91. Schwarz DS, Zamore PD. Why do miRNAs live in the miRNP? Genes & development. 2002;16(9):1025-31.

92. Pratt AJ, MacRae IJ. The RNA-induced silencing complex: a versatile gene-silencing machine. The Journal of biological chemistry. 2009;284(27):17897-901.

93. Lim LP, Lau NC, Garrett-Engele P, Grimson A, Schelter JM, Castle J, et al. Microarray analysis shows that some microRNAs downregulate large numbers of target mRNAs. Nature. 2005;433(7027):769-73.

94. Murchison EP, Hannon GJ. miRNAs on the move: miRNA biogenesis and the RNAi machinery. Current opinion in cell biology. 2004;16(3):223-9.

95. Jing Q, Huang S, Guth S, Zarubin T, Motoyama A, Chen J, et al. Involvement of microRNA in AU-rich element-mediated mRNA instability. Cell. 2005;120(5):623-34.

96. Jiang Q, Wang Y, Hao Y, Juan L, Teng M, Zhang X, et al. miR2Disease: a manually curated database for microRNA deregulation in human disease. Nucleic acids research. 2009;37(Database issue):D98-104.

97. de Pontual L, Yao E, Callier P, Faivre L, Drouin V, Cariou S, et al. Germline deletion of the miR-17 approximately 92 cluster causes skeletal and growth defects in humans. Nature genetics. 2011;43(10):1026-30.

98. Hughes AE, Bradley DT, Campbell M, Lechner J, Dash DP, Simpson DA, et al. Mutation altering the miR-184 seed region causes familial keratoconus with cataract. American journal of human genetics. 2011;89(5):628-33.

99. Mencia A, Modamio-Hoybjor S, Redshaw N, Morin M, Mayo-Merino F, Olavarrieta L, et al. Mutations in the seed region of human miR-96 are responsible for nonsyndromic progressive hearing loss. Nature genetics. 2009;41(5):609-13.

100. Vosa U, Vooder T, Kolde R, Fischer K, Valk K, Tonisson N, et al. Identification of miR-374a as a prognostic marker for survival in patients with early-stage nonsmall cell lung cancer. Genes, chromosomes & cancer. 2011;50(10):812-22.

101. Akcakaya P, Ekelund S, Kolosenko I, Caramuta S, Ozata DM, Xie H, et al. miR-185 and miR-133b deregulation is associated with overall survival and metastasis in colorectal cancer. International journal of oncology. 2011;39(2):311-8.

102. Jones K, Nourse JP, Keane C, Bhatnagar A, Gandhi MK. Plasma microRNA are disease response biomarkers in classical Hodgkin lymphoma. Clinical cancer research : an official journal of the American Association for Cancer Research. 2014;20(1):253-64.

103. Hosseinahli N, Aghapour M, Duijf PHG, Baradaran B. Treating cancer with microRNA replacement therapy: A literature review. Journal of cellular physiology. 2018;233(8):5574-88.

104. Maes OC, Chertkow HM, Wang E, Schipper HM. MicroRNA: Implications for Alzheimer Disease and other Human CNS Disorders. Current genomics. 2009;10(3):154-68.

105. Amin ND, Bai G, Klug JR, Bonanomi D, Pankratz MT, Gifford WD, et al. Loss of motoneuron-specific microRNA-218 causes systemic neuromuscular failure. Science. 2015;350(6267):1525-9.

106. Beveridge NJ, Gardiner E, Carroll AP, Tooney PA, Cairns MJ. Schizophrenia is associated with an increase in cortical microRNA biogenesis. Molecular psychiatry. 2010;15(12):1176-89.

107. Hommers LG, Domschke K, Deckert J. Heterogeneity and individuality: microRNAs in mental disorders. Journal of neural transmission. 2015;122(1):79-97.

108. Schratt G. microRNAs at the synapse. Nature reviews Neuroscience. 2009;10(12):842-9.

109. Romao JM, Jin W, Dodson MV, Hausman GJ, Moore SS, Guan LL. MicroRNA regulation in mammalian adipogenesis. Experimental biology and medicine. 2011;236(9):997-1004.

110. Skarn M, Namlos HM, Noordhuis P, Wang MY, Meza-Zepeda LA, Myklebost O. Adipocyte differentiation of human bone marrow-derived stromal cells is modulated by microRNA-155, microRNA-221, and microRNA-222. Stem cells and development. 2012;21(6):873-83.

111. Zuo Y, Qiang L, Farmer SR. Activation of CCAAT/enhancer-binding protein (C/EBP) alpha expression by C/EBP beta during adipogenesis requires a peroxisome proliferator-activated receptor-gamma-associated repression of HDAC1 at the C/ebp alpha gene promoter. The Journal of biological chemistry. 2006;281(12):7960-7.

112. Frost RJ, Olson EN. Control of glucose homeostasis and insulin sensitivity by the Let-7 family of microRNAs. Proceedings of the National Academy of Sciences of the United States of America. 2011;108(52):21075-80.

113. Jun-Hao ET, Gupta RR, Shyh-Chang N. Lin28 and let-7 in the Metabolic Physiology of Aging. Trends in endocrinology and metabolism: TEM. 2016;27(3):132-41.

114. Zhu H, Shyh-Chang N, Segre AV, Shinoda G, Shah SP, Einhorn WS, et al. The Lin28/let-7 axis regulates glucose metabolism. Cell. 2011;147(1):81-94.

115. Ulbing M, Kirsch AH, Leber B, Lemesch S, Munzker J, Schweighofer N, et al. MicroRNAs 223-3p and 93-5p in patients with chronic kidney disease before and after renal transplantation. Bone. 2017;95:115-23.

116. Sharma S, Liu J, Wei J, Yuan H, Zhang T, Bishopric NH. Repression of miR-142 by p300 and MAPK is required for survival signalling via gp130 during adaptive hypertrophy. EMBO molecular medicine. 2012;4(7):617-32.

117. Kim K, Yang DK, Kim S, Kang H. miR-142-3p Is a Regulator of the TGFbeta-Mediated Vascular Smooth Muscle Cell Phenotype. Journal of cellular biochemistry. 2015;116(10):2325-33.

118. Anglicheau D, Sharma VK, Ding R, Hummel A, Snopkowski C, Dadhania D, et al. MicroRNA expression profiles predictive of human renal allograft status. Proceedings of the National Academy of Sciences of the United States of America. 2009;106(13):5330-5.

119. Coussens LM, Werb Z. Inflammation and cancer. Nature. 2002;420(6917):860-7.

120. Esteller M. Non-coding RNAs in human disease. Nature reviews Genetics. 2011;12(12):861-74.

121. Gurha P. MicroRNAs in cardiovascular disease. Current opinion in cardiology. 2016;31(3):249-54.

122. Iorio MV, Croce CM. MicroRNA dysregulation in cancer: diagnostics, monitoring and therapeutics. A comprehensive review. EMBO molecular medicine. 2017;9(6):852.

123. Roush S, Slack FJ. The let-7 family of microRNAs. Trends in cell biology. 2008;18(10):505-16.

124. Rupaimoole R, Slack FJ. MicroRNA therapeutics: towards a new era for the management of cancer and other diseases. Nature reviews Drug discovery. 2017;16(3):203-22.

125. Tili E, Michaille JJ, Croce CM. MicroRNAs play a central role in molecular dysfunctions linking inflammation with cancer. Immunological reviews. 2013;253(1):167-84.

126. Ha M, Kim VN. Regulation of microRNA biogenesis. Nature reviews Molecular cell biology. 2014;15(8):509-24.

127. Lin S, Gregory RI. MicroRNA biogenesis pathways in cancer. Nature reviews Cancer. 2015;15(6):321-33.

128. Bader AG. miR-34 - a microRNA replacement therapy is headed to the clinic. Frontiers in genetics. 2012;3:120.

129. Li Z, Rana TM. Therapeutic targeting of microRNAs: current status and future challenges. Nature reviews Drug discovery. 2014;13(8):622-38.

130. Rupaimoole R, Calin GA, Lopez-Berestein G, Sood AK. miRNA Deregulation in Cancer Cells and the Tumor Microenvironment. Cancer discovery. 2016;6(3):235-46.

131. van Rooij E, Kauppinen S. Development of microRNA therapeutics is coming of age. EMBO molecular medicine. 2014;6(7):851-64.

132. Blum JS, Saltzman WM. High loading efficiency and tunable release of plasmid DNA encapsulated in submicron particles fabricated from PLGA conjugated with poly-L-lysine. Journal of controlled release : official journal of the Controlled Release Society. 2008;129(1):66-72.

133. Kulkarni RK, Moore EG, Hegyeli AF, Leonard F. Biodegradable poly(lactic acid) polymers. Journal of biomedical materials research. 1971;5(3):169-81.

134. Yang XZ, Dou S, Sun TM, Mao CQ, Wang HX, Wang J. Systemic delivery of siRNA with cationic lipid assisted PEG-PLA nanoparticles for cancer therapy. Journal of controlled release : official journal of the Controlled Release Society. 2011;156(2):203-11.

135. Trang P, Wiggins JF, Daige CL, Cho C, Omotola M, Brown D, et al. Systemic delivery of tumor suppressor microRNA mimics using a neutral lipid emulsion inhibits lung tumors in mice. Molecular therapy : the journal of the American Society of Gene Therapy. 2011;19(6):1116-22.

136. Landen CN, Jr., Chavez-Reyes A, Bucana C, Schmandt R, Deavers MT, Lopez-Berestein G, et al. Therapeutic EphA2 gene targeting in vivo using neutral liposomal small interfering RNA delivery. Cancer research. 2005;65(15):6910-8.

137. Nishimura M, Jung EJ, Shah MY, Lu C, Spizzo R, Shimizu M, et al. Therapeutic synergy between microRNA and siRNA in ovarian cancer treatment. Cancer discovery. 2013;3(11):1302-15.

138. Joshi HP, Subramanian IV, Schnettler EK, Ghosh G, Rupaimoole R, Evans C, et al. Dynamin 2 along with microRNA-199a reciprocally regulate hypoxia-inducible factors and ovarian cancer metastasis. Proceedings of the National Academy of Sciences of the United States of America. 2014;111(14):5331-6.

139. Ozpolat B, Sood AK, Lopez-Berestein G. Nanomedicine based approaches for the delivery of siRNA in cancer. Journal of internal medicine. 2010;267(1):44-53.

140. Rupaimoole R, Ivan C, Yang D, Gharpure KM, Wu SY, Pecot CV, et al. Hypoxia-upregulated microRNA-630 targets Dicer, leading to increased tumor progression. Oncogene. 2016;35(33):4312-20.

141. Pecot CV, Rupaimoole R, Yang D, Akbani R, Ivan C, Lu C, et al. Tumour angiogenesis regulation by the miR-200 family. Nature communications. 2013;4:2427.

142. Liu G, Yang D, Rupaimoole R, Pecot CV, Sun Y, Mangala LS, et al. Augmentation of response to chemotherapy by microRNA-506 through regulation of RAD51 in serous ovarian cancers. Journal of the National Cancer Institute. 2015;107(7).

143. MacDiarmid JA, Mugridge NB, Weiss JC, Phillips L, Burn AL, Paulin RP, et al. Bacterially derived 400 nm particles for encapsulation and cancer cell targeting of chemotherapeutics. Cancer cell. 2007;11(5):431-45.

144. Taylor K, Howard CB, Jones ML, Sedliarou I, MacDiarmid J, Brahmbhatt H, et al. Nanocell targeting using engineered bispecific antibodies. mAbs. 2015;7(1):53-65.

145. Akhtar S, Benter IF. Nonviral delivery of synthetic siRNAs in vivo. The Journal of clinical investigation. 2007;117(12):3623-32.

146. Duncan R, Izzo L. Dendrimer biocompatibility and toxicity. Advanced drug delivery reviews. 2005;57(15):2215-37.

147. Davis ME, Zuckerman JE, Choi CH, Seligson D, Tolcher A, Alabi CA, et al. Evidence of RNAi in humans from systemically administered siRNA via targeted nanoparticles. Nature. 2010;464(7291):1067-70.

148. Gonzalez H, Hwang SJ, Davis ME. New class of polymers for the delivery of macromolecular therapeutics. Bioconjugate chemistry. 1999;10(6):1068-74.

149. Kim SH, Jeong JH, Lee SH, Kim SW, Park TG. PEG conjugated VEGF siRNA for anti-angiogenic gene therapy. Journal of controlled release : official journal of the Controlled Release Society. 2006;116(2):123-9.

150. Ragelle H, Vandermeulen G, Preat V. Chitosan-based siRNA delivery systems. Journal of controlled release : official journal of the Controlled Release Society. 2013;172(1):207-18.

151. Nair JK, Willoughby JL, Chan A, Charisse K, Alam MR, Wang Q, et al. Multivalent N-acetylgalactosamine-conjugated siRNA localizes in hepatocytes and elicits robust RNAi-mediated gene silencing. Journal of the American Chemical Society. 2014;136(49):16958-61.

152. Thum T, Gross C, Fiedler J, Fischer T, Kissler S, Bussen M, et al. MicroRNA-21 contributes to myocardial disease by stimulating MAP kinase signalling in fibroblasts. Nature. 2008;456(7224):980-4.

153. Boettger T, Beetz N, Kostin S, Schneider J, Kruger M, Hein L, et al. Acquisition of the contractile phenotype by murine arterial smooth muscle cells depends on the Mir143/145 gene cluster. The Journal of clinical investigation. 2009;119(9):2634-47.

154. Cordes KR, Sheehy NT, White MP, Berry EC, Morton SU, Muth AN, et al. miR-145 and miR-143 regulate smooth muscle cell fate and plasticity. Nature. 2009;460(7256):705-10.

155. Davis-Dusenbery BN, Chan MC, Reno KE, Weisman AS, Layne MD, Lagna G, et al. down-regulation of Kruppel-like factor-4 (KLF4) by microRNA-143/145 is critical for modulation of vascular smooth muscle cell phenotype by transforming growth factor-beta and bone morphogenetic protein 4. The Journal of biological chemistry. 2011;286(32):28097-110.

156. Xin M, Small EM, Sutherland LB, Qi X, McAnally J, Plato CF, et al. MicroRNAs miR-143 and miR-145 modulate cytoskeletal dynamics and responsiveness of smooth muscle cells to injury. Genes & development. 2009;23(18):2166-78.

157. Ikeda S, He A, Kong SW, Lu J, Bejar R, Bodyak N, et al. MicroRNA-1 negatively regulates expression of the hypertrophy-associated calmodulin and Mef2a genes. Molecular and cellular biology. 2009;29(8):2193-204.

158. Shan ZX, Lin QX, Fu YH, Deng CY, Zhou ZL, Zhu JN, et al. Upregulated expression of miR-1/miR-206 in a rat model of myocardial infarction. Biochemical and biophysical research communications. 2009;381(4):597-601.

159. Grueter CE, van Rooij E, Johnson BA, DeLeon SM, Sutherland LB, Qi X, et al. A cardiac microRNA governs systemic energy homeostasis by regulation of MED13. Cell. 2012;149(3):671-83.

160. Montgomery RL, Hullinger TG, Semus HM, Dickinson BA, Seto AG, Lynch JM, et al. Therapeutic inhibition of miR-208a improves cardiac function and survival during heart failure. Circulation. 2011;124(14):1537-47.

161. Davalos A, Goedeke L, Smibert P, Ramirez CM, Warrier NP, Andreo U, et al. miR-33a/b contribute to the regulation of fatty acid metabolism and insulin signaling. Proceedings of the National Academy of Sciences of the United States of America. 2011;108(22):9232-7.

162. Rayner KJ, Esau CC, Hussain FN, McDaniel AL, Marshall SM, van Gils JM, et al. Inhibition of miR-33a/b in non-human primates raises plasma HDL and lowers VLDL triglycerides. Nature. 2011;478(7369):404-7.

163. Rayner KJ, Suarez Y, Davalos A, Parathath S, Fitzgerald ML, Tamehiro N, et al. MiR-33 contributes to the regulation of cholesterol homeostasis. Science. 2010;328(5985):1570-3.

164. Taibi F, Metzinger-Le Meuth V, M'Baya-Moutoula E, Djelouat M, Louvet L, Bugnicourt JM, et al. Possible involvement of microRNAs in vascular damage in experimental chronic kidney disease. Biochimica et biophysica acta. 2014;1842(1):88-98.

165. Wiese CB, Zhong J, Xu ZQ, Zhang Y, Ramirez Solano MA, Zhu W, et al. Dual inhibition of endothelial miR-92a-3p and miR-489-3p reduces renal injury-associated atherosclerosis. Atherosclerosis. 2019;282:121-31.

166. Eller P, Hochegger K, Feuchtner GM, Zitt E, Tancevski I, Ritsch A, et al. Impact of ENPP1 genotype on arterial calcification in patients with end-stage renal failure. Nephrology, dialysis, transplantation : official publication of the European Dialysis and Transplant Association - European Renal Association. 2008;23(1):321-7.

167. Kirsch AH, Smaczny N, Riegelbauer V, Sedej S, Hofmeister A, Stojakovic T, et al. Regulatory T cells improve nephrocalcinosis but not dystrophic cardiac calcinosis in DBA/2 mice. The American journal of pathology. 2013;183(2):382-90.

168. Kirsch AH, Kirsch A, Artinger K, Schabhuttl C, Goessler W, Klymiuk I, et al. Heterogeneous susceptibility for uraemic media calcification and concomitant inflammation within the arterial tree. Nephrology, dialysis, transplantation : official publication of the European Dialysis and Transplant Association - European Renal Association. 2015;30(12):1995-2005.

169. Eller P, Eller K, Kirsch AH, Patsch JJ, Wolf AM, Tagwerker A, et al. A murine model of phosphate nephropathy. The American journal of pathology. 2011;178(5):1999-2006.

170. Schroder K, Zhang M, Benkhoff S, Mieth A, Pliquett R, Kosowski J, et al. Nox4 is a protective reactive oxygen species generating vascular NADPH oxidase. Circulation research. 2012;110(9):1217-25.

171. Rao SP, Riederer M, Lechleitner M, Hermansson M, Desoye G, Hallstrom S, et al. Acyl chain-dependent effect of lysophosphatidylcholine on endothelium-dependent vasorelaxation. PloS one. 2013;8(5):e65155.

172. Kozina A, Opresnik S, Wong MS, Hallstrom S, Graier WF, Malli R, et al. Oleoyl-lysophosphatidylcholine limits endothelial nitric oxide bioavailability by induction of reactive oxygen species. PloS one. 2014;9(11):e113443.

173. Rivkin N, Chapnik E, Mildner A, Barshtein G, Porat Z, Kartvelishvily E, et al. Erythrocyte survival is controlled by microRNA-142. Haematologica. 2017;102(4):676-85.

174. Sharma S. Immunomodulation: A definitive role of microRNA-142. Developmental and comparative immunology. 2017;77:150-6.

175. Shrestha A, Mukhametshina RT, Taghizadeh S, Vasquez-Pacheco E, Cabrera-Fuentes H, Rizvanov A, et al. MicroRNA-142 is a multifaceted regulator in organogenesis, homeostasis, and disease. Developmental dynamics : an official publication of the American Association of Anatomists. 2017;246(4):285-90.

176. Furchgott RF, Zawadzki JV. The obligatory role of endothelial cells in the relaxation of arterial smooth muscle by acetylcholine. Nature. 1980;288(5789):373-6.

177. Cheng D, Li J, Zhang L, Hu L. miR-142-5p suppresses proliferation and promotes apoptosis of human osteosarcoma cell line, HOS, by targeting PLA2G16 through the ERK1/2 signaling pathway. Oncology letters. 2019;17(1):1363-71.

178. Han GY, Cui JH, Liang S, Li HL. Increased miR-142 and decreased DJ-1 enhance the sensitivity of pancreatic cancer cell to adriamycin. European review for medical and pharmacological sciences. 2018;22(22):7696-703.

179. Li X, Chen W, Jin Y, Xue R, Su J, Mu Z, et al. miR-142-5p enhances cisplatin-induced apoptosis in ovarian cancer cells by targeting multiple anti-apoptotic genes. Biochemical pharmacology. 2019;161:98-112.

180. Mansoori B, Mohammadi A, Gjerstorff MF, Shirjang S, Asadzadeh Z, Khaze V, et al. miR-142-3p is a tumor suppressor that inhibits estrogen receptor expression in ER-positive breast cancer. Journal of cellular physiology. 2019.

181. Naseri Z, Oskuee RK, Jaafari MR, Forouzandeh Moghadam M. Exosome-mediated delivery of functionally active miRNA-142-3p inhibitor reduces tumorigenicity of breast cancer in vitro and in vivo. International journal of nanomedicine. 2018;13:7727-47.

182. Ou ZL, Zhang M, Ji LD, Luo Z, Han T, Lu YB, et al. Long noncoding RNA FEZF1-AS1 predicts poor prognosis and modulates pancreatic cancer cell proliferation and invasion through miR-142/HIF-1alpha and miR-133a/EGFR upon hypoxia/normoxia. Journal of cellular physiology. 2019.

183. Su Y, Wang J, Ma Z, Gong W, Yu L. miR-142 Suppresses Endometrial Cancer Proliferation In Vitro and In Vivo by Targeting Cyclin D1. DNA and cell biology. 2019;38(2):144-50.

184. Zhang HW, Li H, Yan H, Liu BL. MicroRNA-142 promotes the expression of eNOS in human peripheral blood-derived endothelial progenitor cells in vitro. European review for medical and pharmacological sciences. 2016;20(19):4167-75.

185. Choe N, Kwon DH, Shin S, Kim YS, Kim YK, Kim J, et al. The microRNA miR-124 inhibits vascular smooth muscle cell proliferation by targeting S100 calcium-binding protein A4 (S100A4). FEBS letters. 2017;591(7):1041-52.

186. Cui RR, Li SJ, Liu LJ, Yi L, Liang QH, Zhu X, et al. MicroRNA-204 regulates vascular smooth muscle cell calcification in vitro and in vivo. Cardiovascular research. 2012;96(2):320-9.

187. Du Y, Gao C, Liu Z, Wang L, Liu B, He F, et al. Upregulation of a disintegrin and metalloproteinase with thrombospondin motifs-7 by miR-29 repression mediates vascular smooth muscle calcification. Arteriosclerosis, thrombosis, and vascular biology. 2012;32(11):2580-8.

188. Liao XB, Zhang ZY, Yuan K, Liu Y, Feng X, Cui RR, et al. MiR-133a modulates osteogenic differentiation of vascular smooth muscle cells. Endocrinology. 2013;154(9):3344-52.

189. Panizo S, Naves-Diaz M, Carrillo-Lopez N, Martinez-Arias L, Fernandez-Martin JL, Ruiz-Torres MP, et al. MicroRNAs 29b, 133b, and 211 Regulate Vascular Smooth Muscle Calcification Mediated by High Phosphorus. Journal of the American Society of Nephrology : JASN. 2016;27(3):824-34.

190. Qiao W, Chen L, Zhang M. MicroRNA-205 regulates the calcification and osteoblastic differentiation of vascular smooth muscle cells. Cellular physiology and biochemistry : international journal of experimental cellular physiology, biochemistry, and pharmacology. 2014;33(6):1945-53.

191. Yanagawa B, Lovren F, Pan Y, Garg V, Quan A, Tang G, et al. miRNA-141 is a novel regulator of BMP-2-mediated calcification in aortic stenosis. The Journal of thoracic and cardiovascular surgery. 2012;144(1):256-62.

192. Goettsch C, Rauner M, Pacyna N, Hempel U, Bornstein SR, Hofbauer LC. miR-125b regulates calcification of vascular smooth muscle cells. The American journal of pathology. 2011;179(4):1594-600.

193. Zheng S, Zhang S, Song Y, Guo W, Zhai W, Qiu X, et al. MicroRNA-297a regulates vascular calcification by targeting fibroblast growth factor 23. Iranian journal of basic medical sciences. 2016;19(12):1331-6.

194. Shang F, Wang SC, Hsu CY, Miao Y, Martin M, Yin Y, et al. MicroRNA-92a Mediates Endothelial Dysfunction in CKD. Journal of the American Society of Nephrology : JASN. 2017;28(11):3251-61.